5-1979

The Effects of Bridging Ligands on Anodic Stripping Voltammetric Analysis

Larry Beasley
Western Kentucky University

Beasley,

Larry Michael

1979

AUTHORIZATION FOR USE OF THESIS

Permission is hereby

☒ granted to the Western Kentucky University Library to make, or allow to be made photocopies, microfilm or other copies of this thesis for appropriate research or scholarly purposes.

☐ reserved to the author for the making of any copies of this thesis except for brief sections for research or scholarly purposes.

Signed J. Michael Beasley

Date 9/24/79

Please place an "X" in the appropriate box.

This form will be filed with the original of the thesis and will control future use of the thesis.

THE EFFECTS OF BRIDGING LIGANDS ON ANODIC STRIPPING VOLTAMMETRIC ANALYSIS

Recommended May 23, 1979
(Date)

John T. Riley
Director of Thesis

Curtis C. Wilkins

David R. Kaufman

Approved July 31, 1979
(Date)

Elmer Gray
Dean of the Graduate College

THE EFFECTS OF BRIDGING LIGANDS ON ANODIC STRIPPING VOLTAMMETRIC ANALYSIS

A Thesis

Presented to

the Faculty of the Department of Chemistry

Western Kentucky University

Bowling Green, Kentucky

In Partial Fulfillment

of the Requirements for the Degree

Master of Science

by

Larry Michael Beasley

May 1979

ACKNOWLEDGEMENTS

I wish to acknowledge my gratitude to the faculty of Western Kentucky University's Chemistry Department, particularly my research committee; Dr. John T. Riley, Dr. Curtis C. Wilkins, and Dr. David R. Hartman; also Mr. C. M. Wilkerson for his help on the synthesis of chromium(III), my wife, and our child who patiently delayed arriving until this thesis was written.

BIOGRAPHICAL SKETCH

LARRY MICHAEL BEASLEY (1948-)

Born [redacted] in Sylacauga, Alabama. Moved to an island off the coast of Florida in the 1950's where he remained until 1968, graduating from Edison Junior College with an A.A. degree. Attended the University of Washington and later Western Kentucky University where a B.S. degree in Chemistry (Math minor) was received in 1977. Enrolled in Western Kentucky University's Master of Science program in 1977 and graduated in 1979, tired and hungry.

TABLE OF CONTENTS

LIST OF FIGURES

LIST OF FIGURES (Continued)

LIST OF TABLES

Table

THE EFFECTS OF BRIDGING LIGANDS ON ANODIC STRIPPING VOLTAMMETRIC ANALYSIS

Larry Michael Beasley May 1979 67 pages

Directed by: John T. Riley, C. C. Wilkins, David R. Hartman

Department of Chemistry Western Kentucky University

Anodic stripping voltammetry (ASV) is an electroanalytical method used in the determination of trace metals in solutions volumes of 20 milliliters or less. Generally, 10^{-6} M concentrations are routinely analyzed.

The analysis of Zn(II), Cd(II), and Cr(III) by ASV was investigated, and the effects of introducing the bridging ligands, cyanide and thiocyanate into solutions of these metal ions was examined. These effects include a cathodic shift in the reduction potentials of the metals, and ASV signal changes ranging from small increases in peak currents to a total loss of peak-current signals, depending on the concentration of the ligand added.

I. INTRODUCTION - ANODIC STRIPPING VOLTAMMETRY

A. History

Anodic stripping voltammetry (ASV) was first attempted in 1931 by Zbinden[1] when the amount of copper he had plated onto a platinum electrode for an electrogravimetric determination was too small to be weighed accurately. He then devised a method to circumvent this problem by reversing the current which effectively stripped the metal off the platinum wire electrode. The current consumed during this process enabled a quantitative determination of the amount of copper present and the voltage at which the copper was stripped from the electrode could be used to identify that element. This process, anodic stripping voltammetry, was thus begun as a new analytical technique.

Not much work was done in this new field and little interest was shown until it became revitalized in the 1950's when the use of mercury electrodes were proposed.[2,3] During the 1960's, anodic stripping voltammetry became well documented for the mercury film electrodes (MFE) and the hanging drop mercury electrodes (HDME). Currently, many new techniques are being tried to improve its use. The research reported in this thesis represents an attempt to improve the sensitivity of chromium(III), zinc(II), and cadmium(II) through the addition of cyanide and thiocyante bridging ligands.

B. Method

The method of ASV involves essentially three steps: an electrolytic concentration, a rest period, and finally the stripping process. The first of these, the electrolytic concentration step, is performed at a constant potential. A potential is chosen that is cathodic (more negative) than the reduction potentials of the metals of interest. A constant potential fitting this criterion is then applied which effectively plates (reduces) all the metals in the dilute solution onto the electrode of choice. The choice of electrode depends on the metals to be analyzed and their respective range of reduction potentials. The solution is stirred at a constant rate during this electrolytic concentration step to insure a constant supply of depolarizer from the bulk of the solution. When stationary electrodes are used, the stirring is stopped after a certain length of time and the entire solution is allowed to become "still." The flux of the metals or substances being plated on the electrode diminishes and results in the value of the electrolytic current falling rapidly to the value of the stationary diffusion current. Following this "resting," or quiescent period, the voltage is scanned anodically (in the positive direction) and the plated substances are consequently stripped (oxidized) out of the electrode back to the solution at a potential corresponding to their oxidation potential.

The current consumed during the stripping process is recorded with respect to that particular voltage where such a consumption occurs. This requires that the electrode potential change linearly with time for the best possible measuring

conditions. The current consumption of a particular species produces a peak on the resulting polarization curve, the position of which (E_p) is characteristic of the given substance and the height of this peak (or its area) is proportional to its concentration in the solution, when constant electrolytic (potential) concentration conditions are utilized.

ASV essentially has two methods of stripping. The first type involves the complete electrolysis of the substance from the solution and monitoring of the current until this dissolution is complete. This method is very precise and accurate under ideal conditions. However, it is rather time consuming, especially if large solution volumes are used. It is therefore an advantage in an analysis to work with a smaller, more reproducible volume where the depolarizer is removed from the solution in a relatively short amount of time.[4] The second method, which is the type used in this research project, involves carrying out the electrolytic concentration under reproducible conditions for a specific length of time. Exactly how this time span was decided upon will be dealt with in a later section. By utilizing a specific period of time, the amount of substance deposited onto the electrode will be a reproducible fraction of the total amount present in the solution. In using this technique one must insure that the mass transport velocity toward the electrode is constant and the electrolytic concentration conditions are such that only 2-3% of the total amount of metal ions in a solution is deposited.[5]

Generally, in ASV work the amount of current flowing at a given potential depends on two main features: the amount of substance to be plated out, and the conditions of the stripping process. The amount of substance to be plated out is a function of the concentration of the substance in the solution, the length of time the concentration step is carried out, the rate of flux of the substance from the bulk of the solution toward the electrode (the stirring rate), the volume and active surface area of the electrode, the species which comprise the solution, and the temperature. The conditions of the stripping process include the rate of polarization, the active surface area of the electrode, and the rate of product transport from the electrode. Should a chemical reaction become involved in the overall electrode process, it will also affect the current flowing due to its rate, the character of the reaction products, and the solubility of the compounds involved.[5]

C. Working Electrodes

The working electrodes employed in an ASV process have become more varied as this electroanalytical technique has been improved. Basically, there are two groups of electrodes, the mercury group and the solid (inert) electrode group.

The mercury group is further subdivided into two divisions, that of the hanging mercury drop electrode (HDME) and the mercury film electrodes (MFE). The HDME involves essentially three parts, a capillary from which a mercury droplet is allowed to hang, some means to provide a vacuum to insure that the drop size may be reproduced accurately (assuring

the same geometries for successive drips), and of course, the mercury. Metals capable of forming amalgams with mercury can be concentrated on a stationary mercury electrode. The mercury drop is usually pressed out of the capillary which is attached to some type of mercury reservoir. As the drop exceeds the edge of the capillary, the surface tension of the mercury inside the capillary stabilizes the drop and prevents it from falling off, provided the drop size is itself not excessive. The HDME is not without its undesirable characteristics. These include the back diffusion of the metals from the solution into the capillary during electrolytic concentration, drop instability for the larger drops (which improve sensitivity owing to their larger active surface area), drop size reproducibility, and the possibility of the mercury reacting with some species in the solution.

The second type of mercury electrode is the mercury film electrode (MFE). These electrodes are prepared by depositing a film of mercury electrolytically onto an inert metal or graphite. The films are quite often only several molecular layers thick. The sensitivity of the MFE is achieved due to a larger surface-to-volume ratio. Further, the MFE can be rotated, usually as a rotating disk electrode. The rotation rate (stirring rate) can be accurately measured, increasing the accuracy of the analysis.

The use of mercury itself imposes some restrictions as far as the range of voltages that may be used is concerned. In meutral solutions the useful range has been reported from

-2.5 volts to +0.2 volts (vs. SCE),[5] or more conservatively -1.8 volts vs. SCE on the cathodic side and 0.0 volts on the anodic side.[6] The positive (anodic) potential limit is due to mercury dissolution from the electrode into the solution. One method used to circumvent this is to employ solid microelectrodes made of Pt, Au or graphite. Normal graphite must be impregnated or used as a graphite paste. The exception is the so-called glassy carbon electrodes. Collectively, these electrodes may be called the second group of working electrodes, the solid (inert) electrodes.

The solid (inert) electrodes normally involve surface film formation during electrolysis and the situation is more complicated. Factors such as the structure and surface energy of the electrode, surface catalytic effects and the structure of the deposit formed, all become important in the formation and dissolution of a surface film. The result of all of these factors is a sensitivity less than the mercury group, but reproducibility is still quite acceptable. To insure reproducibility with an electrode such as the graphite paste electrode (GPE) one must provide a fresh active surface area after each scan of the voltages of interest. This means that the electrode must be removed from the solution after each run, the paste extruded beyond the end of the tube, the old surface removed and the new surface polished before further use. The possibility of the solution penetrating the surface layer and contaminating the reserve supply of paste contained in the electrode tube must be considered. As an example of (GPE) contamination, consider the determination of bromide or bromate.

The bromide is readily dissolved and concentrated in the carbon paste, but it is difficult to strip out quantitatively, leading to contamination of the electrode. If organic solvents are used, there is a possibility of reaction or deactivation of the paste. Another disadvantage of the GPE is the cost of replacing the paste since once it has been used it must be discarded. (With the HDME, one can recover the mercury by distillation.) The advantages of using carbon electrodes are their reasonably high hydrogen overpotential, electrical conductivity, insolubility in mercury and chemical inertness.[6]

One improvement on carbon paste electrodes is the wax impregnated graphite electrode (WIGE). This electrode is less porous and does not allow the analyte solution or the mercury film to penetrate the graphite support. The possibility of contamination is reduced and reproducibility of results using this electrode is improved. However, a non-uniform mercury deposit can occur if the electrode is not polished properly. Experiments designed to evaluate the utility of several types of graphite have been done for ASV so as to match electrodes with the desired analysis.[7] Graphite electrodes generally have a useful range from -0.7v to -1.5v. This means that such electrodes become useful when the oxidative stripping potential of the analyte lies in the positive voltage ranges where utilizing mercury's properties is a disadvantage.

D. Interferences

The interferences of any substance can always be eliminated

by separating the interfering component out of the solution to be analyzed. Other less drastic measures that may be used to improve sensitivity and selectivity are to choose the proper electrode and/or a more suitable electrolytic solution, and to control the applied voltage such that it will plate the metal of interest onto the electrode while leaving interfering species in the solution.

Mercury has a desirable characteristic as an electrode material in that it has a very high hydrogen overvoltage. Consequently, hydrogen evolution, from the reduction of water, does not occur until potentials more negative than -1.5 volts have been reached. Using mercury electrodes allows the reduction of many metal ions in aqueous solutions without the proglem of hydrogen evolution.

Sometimes two different metals are stripped from an electrode at approximately the same potential. This problem is resolved in certain cases by using a stripping solution different from the plating solution. The use of different complexing agents that shift the stripping potentials is often beneficial.[8,9]

II. THEORETICAL CONSIDERATIONS OF ASV

A. Electrodeposition Process

An electrodeposition process is thought to proceed essentially by two different mechanisms. In the first mechanism the electroactive particle is transported toward the electrode surface, while, at the same time, undergoing desolvation. Then it diffuses along the electrode's surface to a site where crystal nucleation has started. Here it undergoes a charge-transfer reaction and complete desolvation. In the second mechanism, the particle diffuses through the solution toward the crystal building site while it is being partially desolvated. The charge-transfer reaction and desolvation both take place at the building site of the crystal lattice, and the particle is incorporated into the crystal lattice.[5] These theories of deposit growth on electrodes are based on the model for crystal growth from vapors.[5, 10-14]

Desolvation is assumed to be of fairly high energy since the electroactive particle is often not directly present in the solution but must be formed from a preceeding chemical reaction. Examples would be $Cd(CN)_3^-$ or $Cd(CN)_2$ which must be formed from $Cd(CN)_4^{2-}$. The chemical reaction rate will then participate in controlling the overall rate of the desolvation to some degree. Adsorption of ions and molecules on the electrode has a considerable influence on the entire

electrodeposition process. For a deposit to start growing, nucleation must occur on the electrode's surface, that is, a cluster of atoms of the substrate (material to be deposited) must achieve a critical size. Two cases are obvious: (1) deposition of the same material which results in two-dimensional nuclei being formed and (2) deposition on a different inert material which results in three-dimensional nuclei being formed. The critical size may be estimated as follows when a three-dimensional nucleus is being formed on an infinitely large planar electrode. The increase in electrochemical potential per particle is given by:[15]

$$\Delta\mu = -n\eta e \qquad \text{(II-1)}$$

where: $\Delta\mu$ = increase in electrochemical potential per particle

n = the particle charge

e = the charge on one electron

η = overvoltage

The overall electrochemical free energy of a nucleus composed of p particles is:

$$\Delta G = -np\eta e + \sigma h p^{2/3} \qquad \text{(II-2)}$$

where: ΔG = overall electrochemical free energy

σ = nucleus surface energy (erg/cm^2) per area

h = proportionality constant

$hp^{2/3}$ = nucleus surface area

Upon examination of these equations an insight is gained as to the spontaneous growth of crystals (or plating) onto an electrode. ΔG increases, passes through a maximum (the critical size of the nucleus), and then decreases as the number of

particles, p, is increased - spontaneous growth takes place. Hence, for the critical nucleus size:

$$\frac{\sigma \Delta G}{\sigma p} = 0 = -n\eta e + 2/3\ hp^{-1/3} \qquad \text{(II-3)}$$

$$P_{crit} = \frac{8\sigma^3 h^3}{27n^3\eta^3 e^3} \qquad \text{(II-4)}$$

$$\Delta G_{max} = \frac{4\sigma^3 h^3}{27n^2\eta^2 e^2} \qquad \text{(II-5)}$$

It is interesting to note that equation (II-4) is analogous to the Gibbs-Kelvin equation for the radius of the critical nucleus in crystallization.

Deposit growth by the surface nucleus mechanism requires fairly large overpotentials. Furthermore, when one layer is finished, a new nucleus must be formed for the process to continue. Experimentally however, it has been found that deposit growth occurs at overvoltages lower than the values for surface nucleus growth. This was explained by assuming a spiral growth by the so-called screw dislocation mechanism.[16,17] This spiral growth is caused instead of planar growth by some dislocation produced by a fault such as foreign particles, a heterogeneous nucleus having an irregular crystal lattice, or, deformations of thin plates (or needles) during the initial stages of growth. Whatever the reason for the screw dislocation (deformation) it is the "step" formation in the plating of the crystal surface which allows the strong attractive forces around it to gather other particles so that successive steps are spiral-like in nature with one complete spiral generating one layer of plating.

In practice the deposition of material from the solution is accompanied by surface diffusion and by the direct discharge of ions at the "active sites" located at the screw dislocations. For mercury electrodes it is assumed that the charge-transfer reaction takes place directly on these active sites. The number of these active sites depends to a certain degree on the electrode potential and on the presence of surface active substances. The overall electrodeposition process is controlled by either the rate of the charge transfer reaction (primarily for mercury electrodes) or the rate of transport of the particles through the interface and surface diffusion. When the particle has reached the electrode surface its charge is partially neutralized and is referred to as an ad-atom which is bound to the electrode by an adsorption bond that has the character of a highly polar chemical bond. An example is the ad-atom charge in silver depostiion which is 30-40% of the normal ionic charge on silver(I).[13]

B. Amalgam Properties

This research employed the HDME and, consequently, an understanding of amalgams is important since the analyte becomes incorporated as an amalgam when it is deposited on the electrode surface. There are four areas which should be studied; the solubility of the metal(s) in mercury, possible interactions between dissolved metals and/or mercury, electrochemical properties of amalgams, and finally amalgamation of metallic films (important to MFE which will be omitted).

It is important that the metals dissolve in the mercury to give reproducible results. Amalgamation can be hindered

by a surface oxide layer on the metal. As an example, the solubility of platinum in mercury is 0.1% W/W at 20°C, but almost no amalgamation occurs when platinum wire with an oxide coating is immersed in pure mercury.

The solubility of metals in mercury depends basically on temperature and atomic number. The dependence of the solubility of metals on atomic number has been investigated, but no satisfactory means of predicting this dependence has been determined.[5, 18] Table 1 gives solubility values of some metals in mercury.[18]

Table 1

Solubility of Metals in Mercury[18]

METAL	TEMPER-ATURE °C	Solubility		METAL	TEMPER-ATURE °C	Solubility	
		%W/W	atom%			%W/W	atom%
Li	25	0.048	1.34	Pu	20	0.0154	0.0127
Na	25	0.57	4.8	Si	20	0.001	0.007
K	25	0.395	2.0	Ge	25	1×10^{-6}	---
Rb	25	1.37	3.15	Sn	20	0.6	1.26
Cs	25	4.0	6.0	Pb	20	1.1	1.1
Cu	20	0.003	0.006	Ti	20	5×10^{-6}	2×10^{-5}
Ag	20	0.035	0.066	Zr	20	0.003	0.007
Au	20	0.1306	0.1329	Sb	20	2.9×10^{-5}	4.7×10^{-5}
Be	100	10^{-6}	2×10^{-5}	Bi	20	1.1	1.1
Mg	17	0.31	2.5	V	20	5×10^{-5}	2×10^{-4}
Ca	25	0.30	1.48	Nb	20	0.001	0.002
Sr	20	1.04	2.34	Cr	20	4×10^{-7}*	---
Ba	20	0.33	0.48	Mo	20	2×10^{-5}	4×10^{-5}
Zn	20	1.99	6.4	W	20	10^{-5}	10^{-5}
Cd	20	5.3	---	Mn	20	0.0018	0.0066
Al	20	0.002	0.015	Fe	20	7×10^{-5}**	---
Ga	20	1.13	3.19	Co	20	8×10^{-5}	---
In	20	57.0	70.3	Ni	20	4.8×10^{-5}	---
Tl	20	42.8	42.6	Ru	20	0.353	0.694
La	25	0.0092	0.0133	Rh	20	0.16	0.311
Ce	20	0.016	---	Pd	20	0.006	0.012
Th	20	0.016	0.014	Ir	20	0.001	0.001
U	20	0.005	0.0042	Pt	24	0.09	0.10

* Cr solubility ranges from 4×10^{-7} to 3.1×10^{-11}

** Fe solubility ranges from 7×10^{-5} to 1.15×10^{-17}

The viscosity of amalgams affects the diffusion of the analyte [metal(s)] dissolving in the mercury and consequently the rate of electrochemical reactions for the HDME. Dilute amalgams have essentially the same viscosity as mercury with a slightly lowered value of surface tension. Mercury at 18°C has a viscosity of 15.575 x 10^3 g/cm-sec and a surface tension of 420 dyne/cm for 0.88 equivalents of Zn/1Hg, and 406 for 0.82 equivalents of Cd/1 Hg.

The diffusion coefficients of some metals in mercury, D^{Hg}, are shown in Table 2.[18]

Table 2

Diffusion Coefficients of Metals in Mercury
(D^{Hg} x 10^5 cm^2/sec)[18]

METAL	TEMPERATURE °C	D^{Hg}	METAL	TEMPERATURE °C	D^{Hg}
Li	25	0.93	Ba	7.8	0.60
Na	25	0.86	Zn	25	2.4
K	20	0.66	Pb	25	2.1
Rb	25	0.61	Mn	20	1.84
Cs	25	0.65	Cd	25	2.0
Cu	25	1.06	Hg	20	1.55
Sn	25	1.5	Ga	20	1.64
Bi	25	1.5	In	20	1.42
Ag	25	1.0	Tl	25	1.18
Au	25	0.73	Ge	20	1.71
Ca	10.2	0.62	Sb	20	1.47
Sn	9.4	0.54	Ni	25	2.0

The amalgams that metals form with mercury may be either ionic compounds or metallic systems, although no clear distinction may be drawn between these. Also, many intermetallic compounds with mercury do not correspond to simple stoichiometric ratios. Some differentiation by using phase diagrams has been reported as follows:[5,18,19]

(A) The alkali metals and the alkaline earths form compounds exhibiting a relatively narrow region of homogeneity. That is, these metals form compounds with mercury which have more or less exact compositions (stoichiometrically).

(B) Transition metals of the fourth and eighth groups (d^2 and d^6) are practically insoluble in mercury. Consequently, their amalgams are heterogeneous systems such that they are suspensions of these metal particles in mercury, or sparingly soluble intermetallic compounds.

(C) The metals of the Cu, Zn, Al, Ge, and As groups form almost no intermetallic compounds with mercury.

From these classifications, the pattern that emerges is that strong interactions with mercury are exhibited by metals with unoccupied d-orbitals (group A), whereas, metals with completely filled outer d-orbitals essentially do not interact with mercury (group C). Some metals with incompletely filled d-orbitals (group B) combine in various ways with mercury. For example, metals with an inert s-electron pair such as In and Tl form intermetallic compounds with mercury similar to the alkali metals, and other members of group C do not form such compounds.

C. Chemistry of Selected Metals

This research involved extensive electroanalytical studies with three metal ions, Cr(III), Zn(II), and Cd(II). Due to the nature of the research, the ability of each of the metal ions to form a strong bond with one of the donor atoms in a bridging ligand is an important property to consider. A discussion of the general bonding properties of these three metal ions is therefore appropriate.

Most all chromium(III) compounds are hexacoordinate and, for the most part, relatively stable. Ligand displacement of Cr(II) complexes have half-times, typically, of several hours.[20] The stability of Cr(III) compounds allows them to be isolated as solids or to persist for relatively long periods of time in solution even under thermodynamically unstable conditions. The hexaquo ion $[Cr(H_2O)_6]^{3+}$ has a regular octahedron structure and produces acidic solutions (pKa = 4). The hydroxo ion condenses to give a dimeric hydroxo bridged species:

$$2[Cr(H_2O)_6]^{3+} \underset{+2H^+}{\overset{-2H^+}{\rightleftharpoons}} 2(Cr(H_2O)_5OH]^{2+} \rightleftharpoons [(H_2O)_5Cr\begin{matrix}H\\O\\H\end{matrix}Cr(H_2O_5]^{4+}$$

Should additional base be added, soluble polymeric species are formed taking on a dark green gelled appearance. The $[Cr(H_2O)_2]^{2+}$ species is labile with a half-life for H_2O exchange of about a nanosecond. However, when the Cr(II) ion is oxidized, the Cr(III) product is inert.[21] One further note about Cr(III) is that it has a considerable "hard" character

according to the hard-soft acid base (HSAB) theory in that it forms many complexes with oxygen and nitrogen donor atoms.

Zinc(II) also shows predominately "hard" behavior in that it forms stable complexes with oxygen and nitrogen donor atoms. This metal also complexes with sulfur-containing ligands, such as SCN^-, which indicates its ability to behave as a soft metal also.[22] Generally if Zn(II), Cd(II), or Hg(II) form five-coordinate complexes a trigonal bipyramidal arrangement of the ligands is favored over the square planar configuration. The d^{10} structure is highly symmetrical and the geometry of complexes formed by Zn(II), Cd(II) and Hg(II) is also the most symmetrical possible.[22]

Cadmium(II) is intermediate between "hard" and "soft" whereas mercury(II) is definitely a soft metal. The coordination numbers of Cd(II) are generally 4 and 6. Cadmium(II) is also a d^{10} configuration which means this subshell configuration is characterized by relatively high polarizing power as far as the ion is concerned so that the bonds formed tend to have a significant covalent character. A measure of a metal ion's polarizing power is its electron affinity (the energy released when one or more electrons are acquired to give the atom), which is the same as the ionization energy of the atom but has the opposite sign. An increase in polarizing power of the ion is usually accompanied by a decrease in the coordination number. Although Zn(II), Cd(II), and Hg(II) do form six-coordinate structures, four-coordination is more frequently observed.

D. Mathematical Considerations

The mathematical considerations of ASV are widely documented and also differ slightly depending on which author(s) you read.[5,6,23-31]

First we will consider the electrolytic reduction of a substance, O, to a new form, R, assuming this process to be reversible. We will also assume R is soluble in solution or in mercury (i.e., HDME), and that the potential, E, of the electrode where substance O is reduced is a linear function of time expressed as:

$$E = E_i + vt \qquad \text{(II-6)}$$

where: E = electrode potential where "O" is reduced

E_i = initial electrode potential

v = rate of potential change (volt/sec)

t = time elapsed (sec)

The initial potential, E_i, is adjusted to a value where substance O is not reduced, and as a result we can assume the concentration $C_o(x,o)$ at the beginning of electrolysis is equal to the bulk concentration C° of substance O. Further, the concentration of R before electrolysis is zero, or, $C_R(x,o) = 0$, where x is the distance from the electrode's surface. This means that:

$$C_o(x,t) \longrightarrow C^\circ \text{ as } x \longrightarrow \infty, \text{ and, } C_R(x,t) \longrightarrow 0 \text{ for } x \longrightarrow \infty$$

The first boundary condition is obtained by applying the Nernst Equation,

$$E = E^\circ + \frac{RT}{n\mathcal{F}} \ln \frac{a_o C_o(0,t)}{a_R C_R(0,t)} \qquad \text{(II-7)}$$

or,

$$\frac{C_o(0,t)}{C_R(0,t)} = \frac{a_R}{a_o} e^{\left[\frac{n}{RT}(E_i - E^\circ)\right]} e^{\left[-\frac{n}{RT} vt\right]} \qquad \text{(II-8)}$$

where a is an activity coeff.

$n, \mathfrak{F}$, R, T have the normal meanings

If an amalgam forms, E° becomes the standard potential at unit activity ($a=1$) for substances O, R, when one or both dissolve in mercury. This allows equation (II-8) to be re-written in a more condensed form,

$$\frac{C_o(0,t)}{C_R(0,t)} = \theta e^{(-\sigma t)} \qquad \text{(II-9)}$$

where $$\theta = \frac{a_R}{a_o} e^{\left[\frac{n\mathfrak{F}}{RT}(E_i - E^\circ)\right]} \qquad \text{(II-10)}$$

and $$\sigma = \frac{n\mathfrak{F}}{RT} v \qquad \text{(II-11)}$$

Again, the first boundary condition (II-7) is made assuming that electrochemical equilibrium is achieved at the electrode. The electrode potential, E°, is the standard potential for the couple $O \rightleftharpoons R$, the a's are the activity coefficients, and the other notations have their conventional meanings.

The second boundary condition is achieved by setting the sum of the fluxes of O and R at the electrode surface to zero,

$$D_o\left(\frac{\partial C_o(x,t)}{\partial x}\right)_{x=0} + D_R\left(\frac{\partial C_R(x,t)}{\partial x}\right)_{x=0} = 0 \qquad \text{(II-12)}$$

where D_o, D_R are the diffusion coefficients for substances O and R.

According to Sevcik[32] the flux at the electrode surface is

$$D_o\left(\frac{\partial C_o(x,t)}{\partial x}\right)_{x=0} = \frac{D_o^{1/2}}{2}\left[1 + \frac{1}{\theta}\left(\frac{D_R}{D_o}\right)^{1/2}\right] \cdot \qquad \text{(II-13)}$$

$$C_o \int_o^t \frac{1}{\cosh^2(\sigma/2)(\xi - t_{1/2})} \cdot \frac{1}{\pi^{1/2}(t-\xi)^{1/2}} \cdot \frac{\sigma}{2} d\xi$$

where ξ is an auxiliary integration variable

$t_{1/2}$ is the time corresponding to $E_{1/2}$, where

$$E_{1/2} = E^\circ - \frac{RT}{n\mathcal{F}} \ln\left(\frac{a_R}{a_O}\right)\left(\frac{D_O}{D_R}\right)^{1/2} \qquad \text{(II-14)}$$

$$\text{or,} \quad t_{1/2} = \frac{E_i - E^\circ}{v} + \frac{1}{\sigma} \ln\left(\frac{a_R}{a_O}\right)\left(\frac{D_O}{D_R}\right)^{1/2} \qquad \text{(II-15)}$$

Equation (II-15) is arrived at by manipulations of equations (II-6) and (II-14).

Sevcik evaluated the integral in equation (II-13) by replacing it with a summation whereby the integral was subdivided into L intervals of width W. The following expressions were then substituted into (II-13):

$$(\sigma/2)t = LW \qquad \text{(II-16)}$$

$$(\sigma/2)\xi = pW \qquad \text{(II-17)}$$

$$(\sigma/2)t_{1/2} = L_{1/2}W$$

$$(\sigma/2)dt = W \qquad \text{(II-19)}$$

By combining (II-15) and (II-19):

$$D_O\left(\frac{\partial C_O(x,t)}{\partial x}\right)_{x=0} = D^{1/2}\left[1 + \frac{1}{\theta}\left(\frac{D_R}{D_O}\right)^{1/2}\right] C^\circ \sigma^{1/2} \frac{W^{1/2}}{2^{3/2}\pi^{1/2}} \cdot \sum_{0}^{L} \frac{1}{(L-p)^{1/2}} \cdot \frac{1}{\cosh^2(p - L_{1/2})W} \qquad \text{(II-20)}$$

The current flowing through the cell is obtained by multiplying the flux of the substance O by the product $n\mathcal{F}A$. Equation (II-20) can be simplified since θ (II-10) is much larger than unity and E_i is markedly more anodic than E_O, that is, $(1/\theta)(D_R/D_O)^{1/2}$ may be neglected in comparison to 1 resulting in equation (II-20) being rewritten, where $\dot{\sigma}$ is replaced by its value from $\sigma = \frac{n\mathcal{F}}{RT} v$ (II-11). If we let a function P represent the summation in (II-20):

$$i = \frac{n^{3/2}\mathcal{F}^{3/2}}{R^{1/2}T^{1/2}} AD_O^{1/2} C^\circ v^{1/2} P\left(\frac{n\mathcal{F}}{2RT} vt\right) \qquad \text{(II-21)}$$

Randles[33] solved the same boundary value problem but by a graphic method. His result can be written as in (II-21), however, his values of the function P are somewhat different than Sevcik's. Nicholson[34] performed these calculations also confirming Randles' work.

From equation (II-21) it can be seen that the current, i, is proportional to the function P, yielding current-applied voltage curve shapes as shown below in Fig. 1.

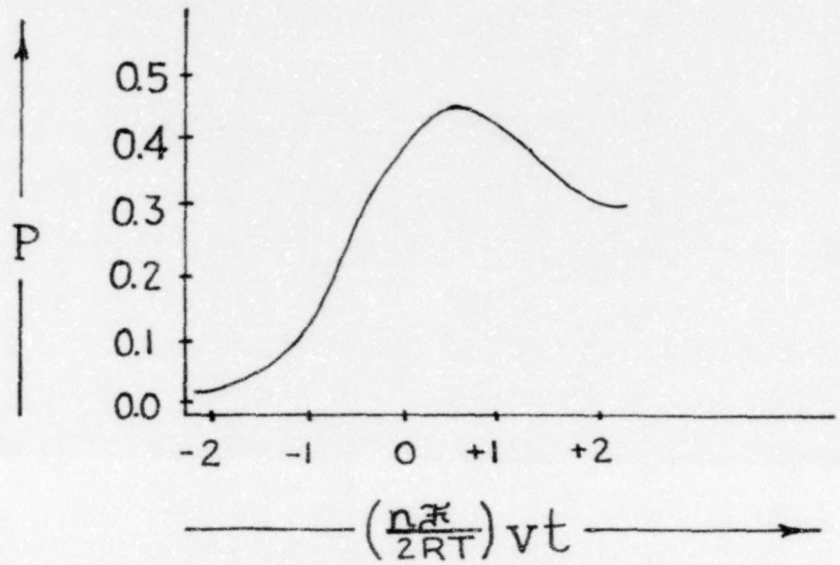

Figure 1. Variations of the function P of equation (II-21)

After the plating (electrolytic concentration) step the voltage output of the power supply varies linearly with time. When the electrolyzed solution is not stirred, and a large excess of supporting electrolyte is present in the test solution, diffusion is the only mode of mass transfer. The current-potential curves obtained in this manner utilizing stationary electrodes, such as the HDME, typically display curves such as Fig. 2.

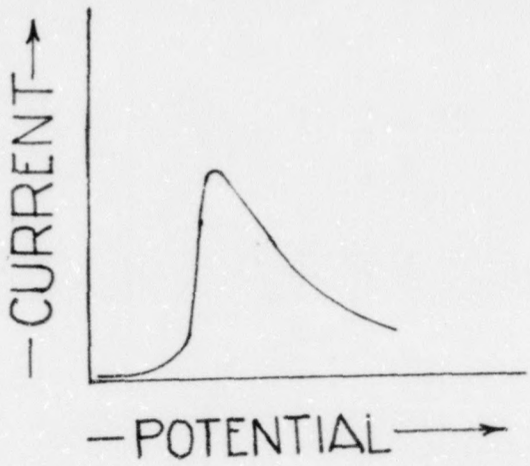

Figure 2. Current-potential curve for continuously changing potential voltammetry (for a stationary working electrode)

Since the voltage applied to the cell varies linearly with time the x-axis (abscissa) can be plotted as either time or potential.

Initially, the rate of reaction is so slow that essentially no current flows through the cell. As voltage varies toward a direction favoring some reaction (redox, etc), the rate of electron transfer at the electrode increases causing the current to increase. The substance reacting at the electrode is progressively removed from the solution in the immediate area of the stationary electrode, thus decreasing the current. The intensity of the maximum current is, again, proportional to the concentration of the oxidized or reduced species.

In the plating step of ASV a constant potential, which is more negative than the reduction potential of any of the metal ions of interest, is applied to the electrolytic cell. Consider the voltage case of the ferricyanide ion at a concentration C° (10^{-3}M) being reduced at a stationary electrode (the cathode) under unstirred conditons. Initially almost all the solution is in the Fe(III) form so that the potential of

the working electrode is given by:

$$E = E^\circ + 0.059 \log \left[\frac{a[Fe(CN)_6]^{3-}}{a[Fe(CN)_6]^{4-}} \right]_{X=0} \qquad \text{(II-22)}$$

Where x = 0 means the activities are taken at the electrode's surface.

E° is the standard potential for

$$[Fe(CN)]^{3-} + e^- \rightleftharpoons [Fe(CN)_6]^{4-}$$

Assuming $a=1$, the above equation becomes

$$E = \text{constant} + 0.059 \log \left[\frac{C[Fe(CN)_6]^{3-}}{C[Fe(CN)_6]^{4-}} \right]_{x=0} \qquad \text{(II-23)}$$

If a large excess of supporting electrolyte is used, the ionic strength of the electrolytic solution is virtually independent of the concentrations of the ferri- and ferrocyanide ions. In this case it is assumed the activity coefficients are independent of the concentrations or $a=1$. When the electrolysis is allowed to proceed, the voltage in the cell must be equal to the applied voltage which means the concentrations of ferri- and ferrocyanide ions are those values dictated by equation (II-23).

Consider a potential whereby the condition of equation (II-24) is satisfied. This occurs when the concentration of

$$\left[\frac{C_{[Fe(CN)_6]^{3-}}}{C_{[Fe(CN)_6]^{4-}}} \right]_{x=0} << 1 \qquad \text{(II-24)}$$

ferricyanide at the electrode surface drops to a value negligible with respect to the bulk concentration, C°, of this substance as soon as electrolysis is begun. This results in a ferricyanide concentration gradient in the immediate vicinity of the electrode (x=0) as the ferricyanide ions diffuse toward

the "active sites" on the electrode. Conversely, the ferrocyanide ions produced by the electrolysis diffuse into the bulk of the solution. As observed in equation (II-24) the concentration of ferricyanide [Fe(III)] at x=0 (the electrode's surface) is constant (approximately zero) during electrolysis since the ferricyanide ions are reduced as rapidly as they are brought to the electrode's surface. This means that the electrolysis current is determined by the rate of diffusion of ferricyanide ions. Furthermore, the electrolysis current observed under these conditions decreases continuously.

When the solution is stirred at a uniform rate, as in the electrolytic concentration step of ASV, more favorable conditions are achieved in that the species being electrolyzed (ferricyanide ion) is continuously brought to the electrode's surface so that a steady current value is obtained. In this case, there exists a steady current for each value of the potential for the working electrode (HDME). The ratios of concentrations of the redox species determine the potential E. If the potential is more positive than E°, the standard potential of the redox couple, by several tenths of a volt the condition which we observe is

$$\left[\frac{C_{[Fe(CN)_6]^{3-}}}{C_{[Fe(CN)_6]^{4-}}}\right]_{x=0} \gg 1 \qquad \text{(II-25)}$$

This condition is satisfied if essentially no ferrocyanide is produced at the electrode's surface (x=0) causing the electrolytic current to be zero. As the potential, E, is made increasingly negative the ratio shown in expression (II-25)

also increases, hence, more ferrocyanide ions are produced at the electrode's surface which causes the current to increase. Eventually an upper plateau is reached where the complete control of the current is governed by mass transport, this current plateau is referred to as the limiting current as shown in Fig. 3.

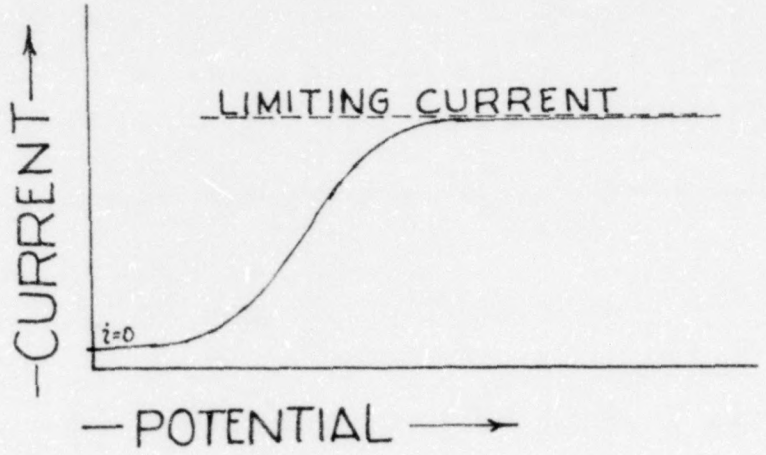

Figure 3. Current-Potential curve in constant voltage voltammetry for a stirred solution.

The rate of mass transfer in electrode processes was first studied by Noyes and Whitney,[35] and later by Nernst[36] who conceived the notion of a diffusion layer (the Nernst diffusion layer, δ_o). This diffusion layer was, according to Nernst, at the surface of the electrode with a thickness of δ_o within which there was no motion (other than linear diffusion) even though the solution was being stirred. The reacting species however, was brought to this layer by the stirring motion and transfer through the layer occurred by ordinary linear diffusion. Furthermore, the concentration of the reacting species is assumed to vary linearly with the distance from the electrode. The concentration gradient at the electrode's

surface is given by

$$\left(\frac{\partial C_o(x)}{\partial x}\right)_{x=0} = \frac{C^o - C_o(o)}{\delta_o} \qquad \text{(II-26)}$$

Where δ_o = reaction layer thickness (diffusion layer)

C^o = bulk concentration of the substance reacting at the electrode

$C_o(0)$ = the concentration of substance O at the electrode's surface

Notice that the concentration of substance O at the electrode surface is written as $C_o(0)$ and not $C_o(0,t)$, as in equation (II-7), since the steady state is assumed to be existing in that the rate of mass transport is constant due to stirring. If the electrochemical reaction is very fast, $C_o(0)$ at the electrode's surface is essentially zero and the gradient is the value of C^o/δ_o. This means that the curve $C_o(x)$ vs x can be replaced by a straight line whose slope is defined by equation (II-26) as pictorially illustrated in Fig. 4.

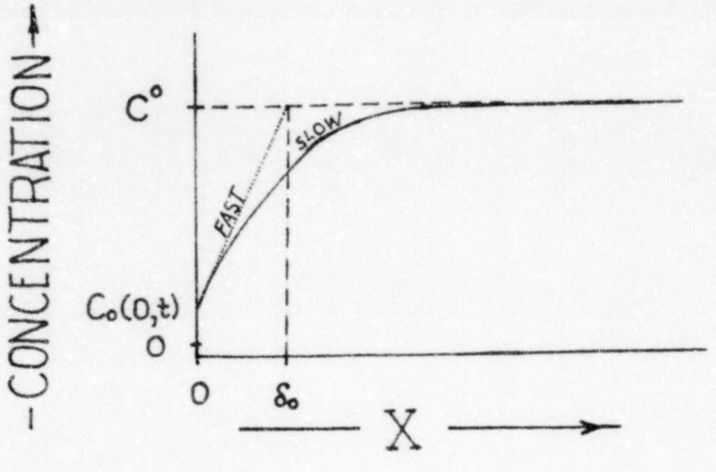

Figure 4. Variations of the concentration of the reacting species with distance from the electrode.

The current for the reduction of substance O can be readily calculated from Fick's first law, and, if one assumes

the effect of migration negligible, that current is

$$i = nFAD_o\left(\frac{\partial C_o(x)}{\partial x}\right)_{x=0} \qquad \text{(II-27)}$$

Where A is the area of the electrode

or, from equation (II-26):

$$i = nFAD_o\left(\frac{C^\circ - C_o(0)}{\delta_o}\right) \qquad \text{(II-28)}$$

Where n is the number of electrons involved in the reaction. The corresponding limiting current, i_L, is given by

$$i_L = nFAD_o\,\frac{C^\circ}{\delta_o} \qquad \text{(II-29)}$$

Hence, the limiting current is proportional to the factors A, D_o, C°, and inversely proportional to δo.

In a reversible process $C_o(0)$ and $C_R(0)$ are related by the Nernst equation as we have already seen in equation (II-7).

$$E = E^\circ + \frac{RT}{nF}\ln\frac{a_o C_o(0,t)}{a_R C_R(0,t)}$$

Now that the origins of the reducing current is clear it is important that we arrive at a value or a means to obtain a value of the maximum current (or peak current), i_p, since this will allow us to calculate the concentration of the reacting species. From equation (II-21) we have plotted the function of P versus (nF/2RT)vt in Fig. 1 and noted that a maximum is indeed observed. The function P, which represented the summation in equation (II-20), exhibits this maximum at a value of 0.452 $sec^{1/2}$, hence the corresponding peak current, i_p, is

$$i_p = 0.452\,\frac{n^{3/2}F^{3/2}}{R^{1/2}T^{1/2}}AD^{1/2}C^\circ V^{1/2} \qquad \text{(II-30)}$$

or, at 25°C

$$i_p = 2.72 \times 10^5 n^{3/2} A D^{1/2} C^{\circ} V^{1/2} \qquad \text{(II-31)}$$

Where C° is the concentration of the analyte in the mercury drop. Equation (II-31) is therefore the expression used in ASV theory to describe the behavior of the HDME. Furthermore, from Fig. 5 one can obtain:

$$E_p = E_{p/2} - 1.1 \frac{RT}{n\mathcal{F}} \qquad \text{(II-32)}$$

Where E_p is the peak potential and $E_{1/2}$ is the half-wave potential.

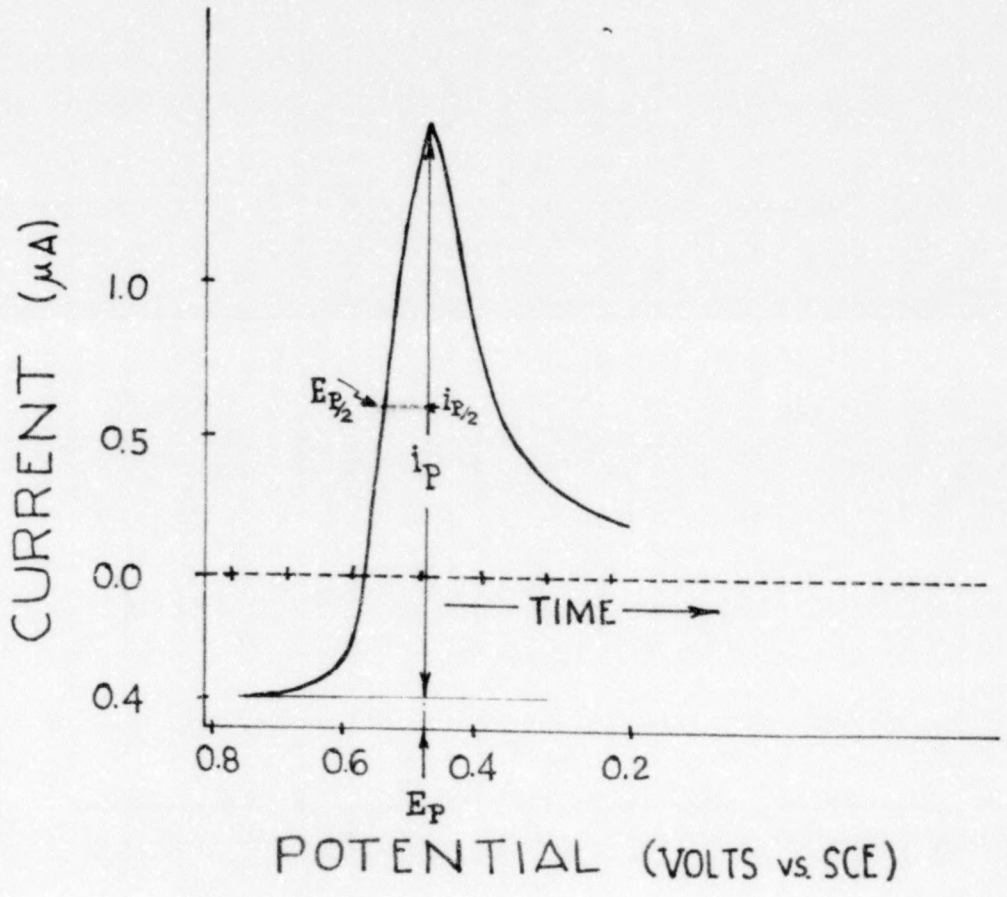

Figure 5. Analyzing features on a typical dissolution curve

E. Outline of Research

The research performed involved selection of electrodes, metals, equipment and conditions most appropriate to an ASV analysis. The HDME was selected since it would cover the widest range of potentials.

The metals chosen were transition metals. Two metals of special interest were Fe(II) and Cr(III) since very little work has been done on these metals with the HDME. Other metals investigated were Zn(II), Ni(II), Cd(II) and Co(II). Some of the metals presented problems in that either they were unsuited to the HDME, or, their potentials for oxidation-reduction exceeded the useful range of the electrode. The goal of the research was to find a method by which transition metals (especially the less electroactive species) could be detected at concentrations lower than presently found in the literature.

Bridging ligands, CN^- and SCN^-, were used as the means to improve sensitivity. In theory, the ligand would attach to the mercury at one end and to a metal in the solution with the other. Since the SCN^- ligand was capable of charge transfer it should have promoted the oxidation-reduction of the metal and lowered its limit of detection.

The optimizing of conditions such as plating time, scan rate, stirring rate and mercury drop size was experimentally determined.

III. EXPERIMENTAL

A. Reagents and Equipment

All the glassware used in this research was rinsed with 1:1 HNO_3 which was followed by rinsing with DI H_2O. The glassware soaked in a 1% EDTA solution overnight showed no more accurate results than that rinsed with 1:1 HNO_3 and DI H_2O immediately after each run.

The reagents employed were Baker reagent grade; KNO_3, KSCN, KCN, KBr, KCl, and H_2SO_4. A primary standard of 99.7% pure $K_2Cr_2O_7$ was utilized in the synthesis of chromium(III) and Harleco atomic absorption standards (1000 ppm) were used as stock solutions in the preparation of all the other metal concentrations (Co, Ni, Zn, Cd, Fe).

The equipment used in the research consisted of the following items. The voltammetry unit, Model CV-1A from Bioanalytical Systems, West Lafayette, Indiana, was connected to an Omnigraphic Model 2122-6-5 recorder from the Houston Instrument Company. The electrolytic cell was a jacketed titration vessel (20 milliliters) from Brinkman Instruments, Inc. A Haake F-junior (FJ and FE) constant temperature circulation pump was used to control the temperature in the cell. The electrodes used were a saturated calomel electrode (Metrohm EA404) and a hanging drop mercury electrode (Metrohm E-410) from Brinkman Instruments, Inc. The auxillary electrode was a platinum wire.

B. The Hanging Drop Mercury Electrode

Perhaps one of the more adventuresome aspects of this research was the mastery of the stubborn hanging drop mercury electrode. It is now much less troublesome and it is my hope that by including this section anyone reading it will be spared weeks of "adventures with the HDME." A schematic diagram of the HDME is shown dissected in Fig. 6.

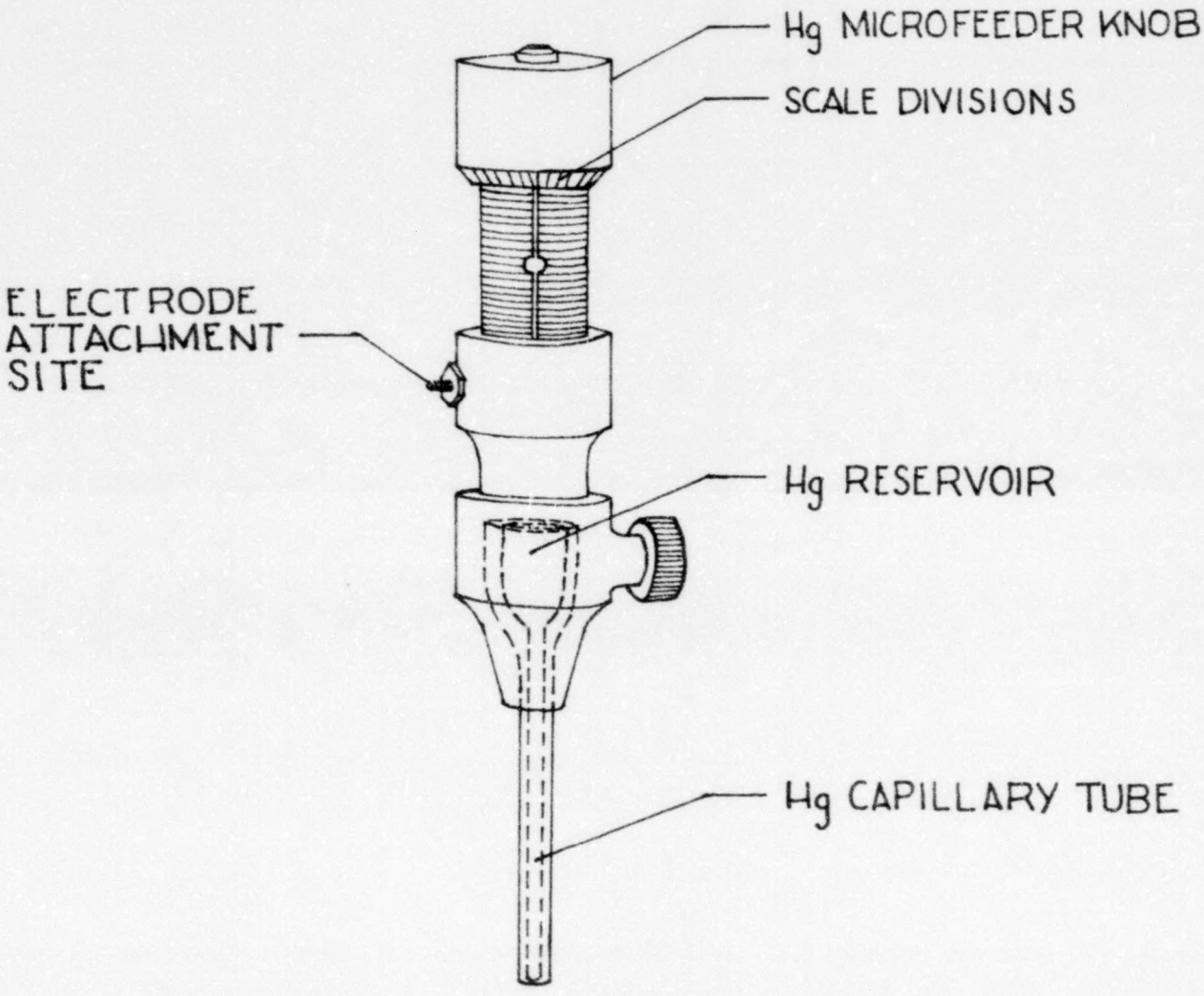

Figure 6. A diagram of the HDME

A problem encountered in using this electrode is loading the mercury and getting all the air out so the drop sizes are

reproducible. According to the operating instructions the reservoir is loaded with a dropper, the electrode reassembled, turned upside down and the top of the mercury microfeeder knob is tapped gently while turning the knob until there are no breaks (air gaps) in the mercury column.[38] This filling method is very time consuming and very little mercury remains in the tube once the process is completed. As a result the electrode must be filled frequently. The method developed to avoid this involves fitting the electrode as described above, then turning the microfeeder knob in until a large drop of mercury is formed on the end of the capillary. The end of the capillary tube is then immersed into the mercury replenishing bottle or vial, and the microfeeder knob turned out, drawing mercury into the reservoir. The HDME can be completely filled by this method so that more uninterrupted runs may be made. To prevent contamination it is best to allow the capillary tube to take up the mercury from the middle of the mercury replenishing pool and not from the sides or bottom of the bottle. Before replenishing the mercury, a substantial amount of mercury must be extruded from the electrode. If back diffusion of reduced species into the mercury column had occurred, the mercury replenishing pool in the bottle would have become contaminated. If the mercury surface is dull, it should be redistilled since the presence of oxides will affect the surface tension of mercury and hence the drop size, leading to poor experimental results. By placing a small volume of distilled water over the surface of the mercury in bottles, its oxidation by air will be inhibited to some degree.

The exact drop sizes for certain scale divisions of the Metrohm E-410 HDME has been determined by optical methods and are listed in Table 3.[38] Storage of the capillary tubes while not in use should be in air [emptied and cleaned].

Table 3

Drop Sizes of the E-410 HDME

Scale Divisions on E-410	Drop Diameter in mm	Drop Surface Area in mm^2
1	0.52	0.86 ± 0.03
2	0.66	1.38 ± 0.04
3	0.76	1.80 ± 0.05
4	0.83	2.22 ± 0.07

C. Preparation of Chromium(III) Standards

An accurately known standard of chromium(III), free of any interferring oxides and ligands was required for this research. There were several unsuccessful attempts to prepare such a standard utilizing chromium metal and acids. Mr. C. M. Wilkerson of the Western Kentucky University Chemistry Department suggested a synthesis from $K_2Cr_2O_7$ which is used as a primary standard in quantitative analysis. The synthesis involved using enough H_2SO_4 (conc.) to dissolve the $K_2Cr_2O_7$ and then using an excess of H_2O_2 to reduce the Cr(VI) to Cr(III). This method was excellent, quick and clean as far as having no residual oxides and unwanted anions.

To prepare a solution of Cr(III) the following reaction applies:

$$K_2Cr_2O_7 + 4H_2SO_4 + 2H_2O_2 \longrightarrow Cr_2(SO_4)_3 + K_2SO_4 + 3\,O_2\uparrow + 6H_2O \quad \text{(IV-1)}$$

The weights and volumes required for the preparation of a 1000 ppm standard solution are as follows: 1.4144 g $K_2Cr_2O_7$ + 1.03 ml 18 M H_2SO_4 + 7-10 ml of 30% H_2O_2 (>tenfold excess). The $K_2Cr_2O_7$ is dissolved in the H_2SO_4; adding a small amount of D.I. H_2O aids the dissolution process. The H_2O_2 is then added and the solution heated for 10 minutes at a temperature high enough (near boiling) to decompose the excess H_2O_2. The resulting solution has a blue-green color. When an insufficient amount of H_2O_2 is used, all the orange-yellow $K_2Cr_2O_7$ is not reduced to Cr(III) and the resulting solution has a green color. The prepared solution used in this research was analyzed for chromium content using atomic absorption spectrophotometry. There was no appreciable difference in chromium content between the prepared Cr(III) standard and an atomic absorption standard of 1000 ppm Cr(VI).

IV. RESULTS AND DISCUSSION

A. Factors Affecting Current-Voltage Curves

A typical voltammogram of current, i, vs. applied potential, E, for a sample in 0.1 M KNO_3 (one of the electrolytic concentrations used in this research) appears in Fig. 7.

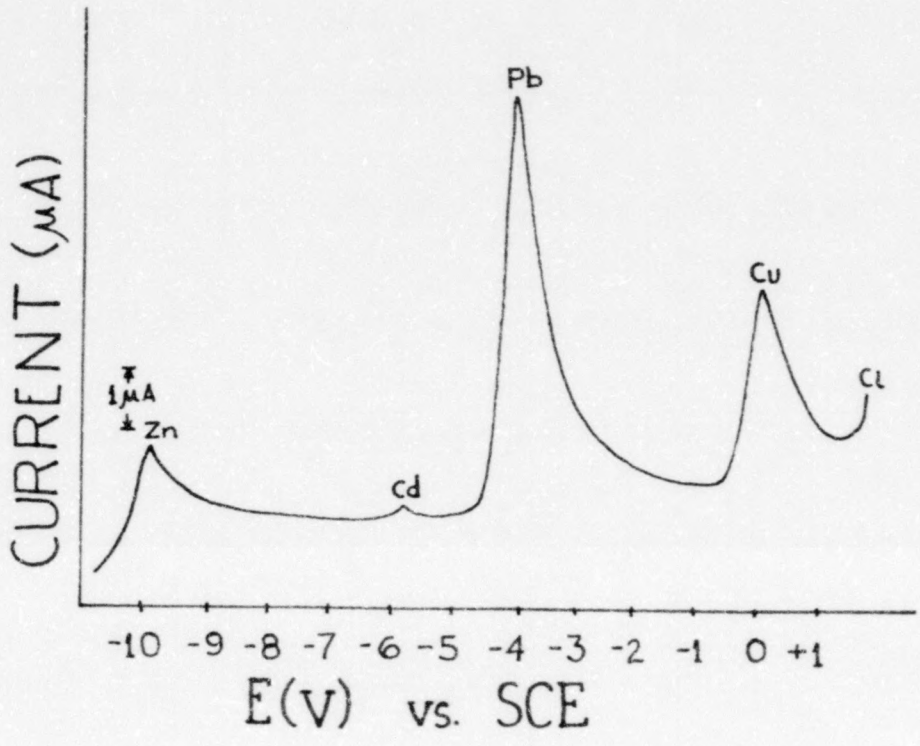

Figure 7. Typical current-voltage curve of a sample in 0.1 M KNO_3[37]

The process of anodic stripping, as mentioned before, is carried out by scanning from an initial voltage, which is more negative than the analyte's reduction potential, through a series of voltages more positive (anodic) until the limit of the electrode is reached. The information that can be obtained from the dissolution curve that results is depicted in Fig. 5. To obtain the peak current, ip, a tangent to the curve is drawn from the cathodic side toward the anodic side. The peak current is then measured as shown in Fig. 5.

There are many factors which affect the character of the dissolution curves in anodic stripping voltammetry. The factors which were examined in this work were the effect of the scanning rate on peak current, stirrer-electrode distance on peak current, size of the mercury drop on peak current, time of the electrolytic concentration step on peak current, pH on curve shape, and finally the effect of bridging ligands on curve shape and peak current.

The effect of scanning rate on peak current is well documented. Generally, as the scanning rate is increased the peak height (current) increases as shown by Fig. 8. It is interesting to note that not only were the peak heights for Cu(II), Pb(II), and Zn(II) increased as the scanning rate was increased, but also the peak potentials for zinc were shifted anodically (Fig. 9). This shift may be caused by the evolution of hydrogen which may build up in the solution with time.

Peak height maximization by optimizing the scan rate does have its limitations since the faster scan rate may exceed the rate of the electrochemical reaction. This occurred in some

of the earlier runs when the scan rates were too fast, which resulted in very unsymmetrical peaks. When the scan rates were decreased, the peaks were well defined. In subsequent runs a scan rate of 50 mv/sec was used, which seemed to yield the best peaks. The peak height appears to be proportional to the square root of the scanning rate.

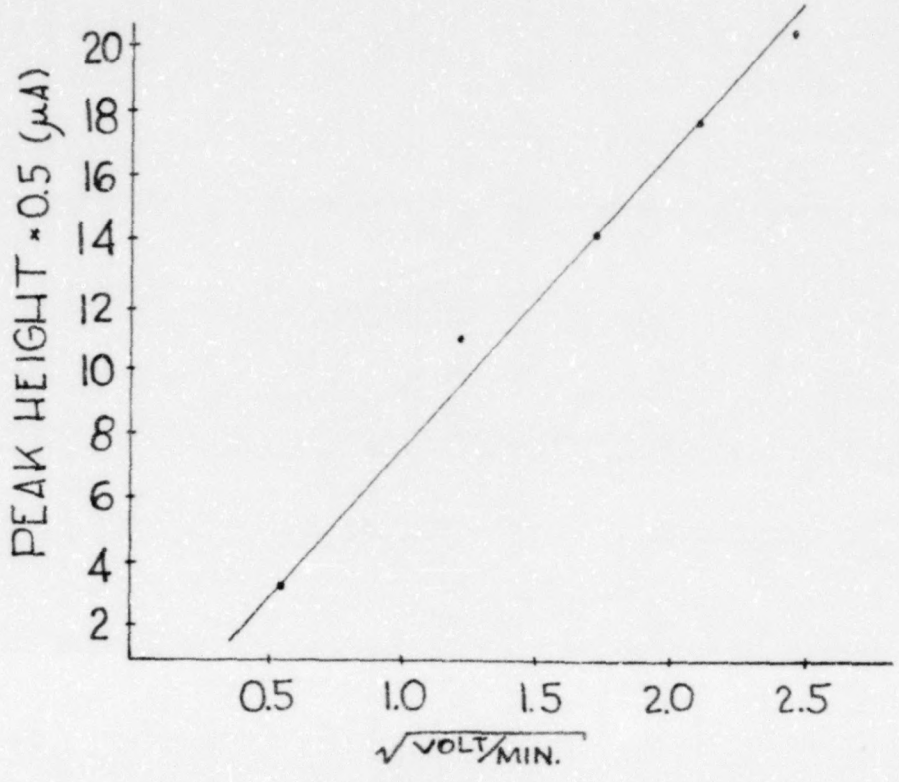

Figure 8. Peak Height vs $\sqrt{\text{scanning rate}}$ for 10 p.p.m. Lead(II) in 0.10 M KNO_3

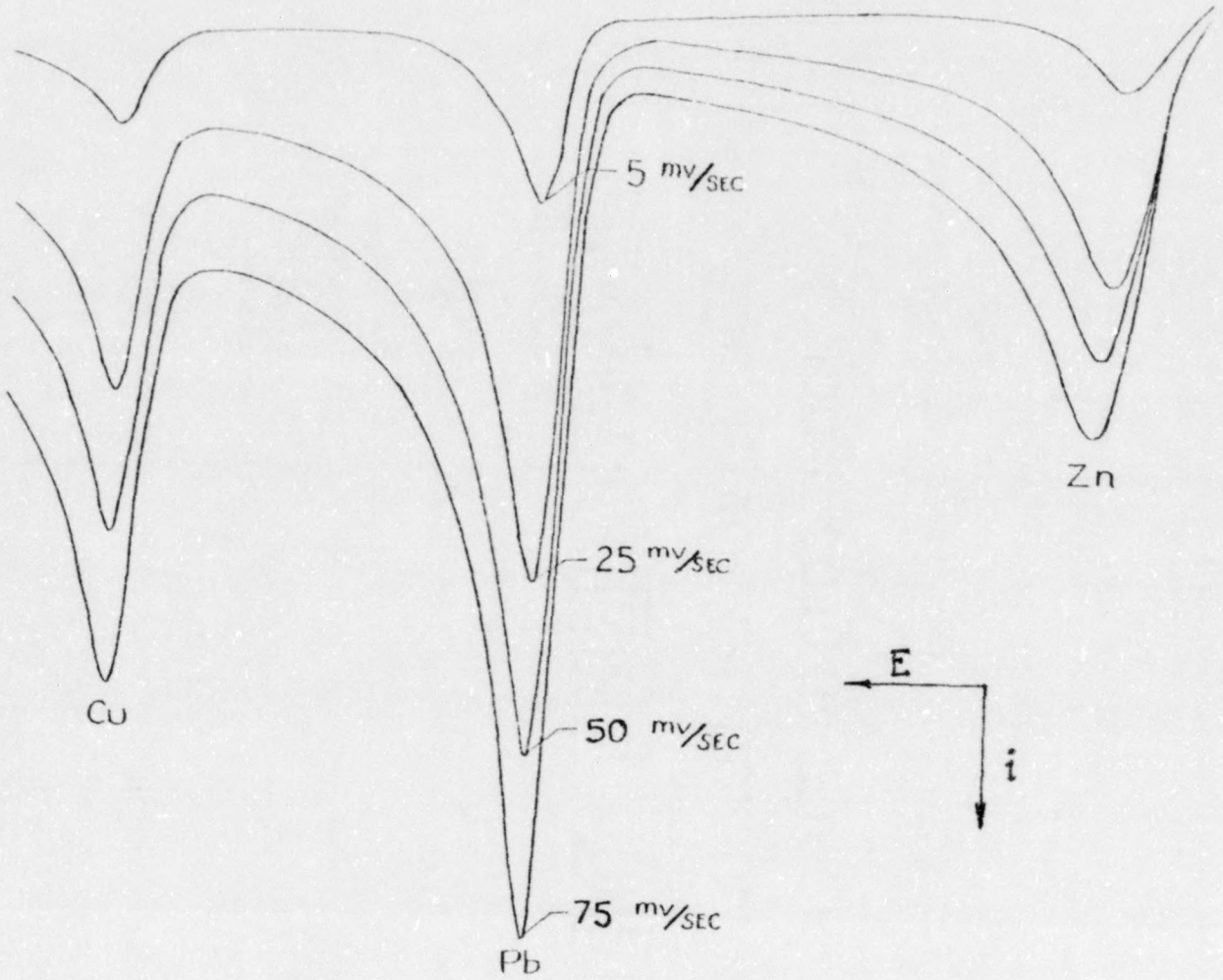

Figure 9. The effect of scan rate on peak current height for 2 ppm Cu(II), Zn(II), and 10 ppm Pb(II) in 0.1 M KNO_3

The stirrer-electrode separation was found by Nikelly and Cooke[3] to also have an effect on peak height (Fig. 10).

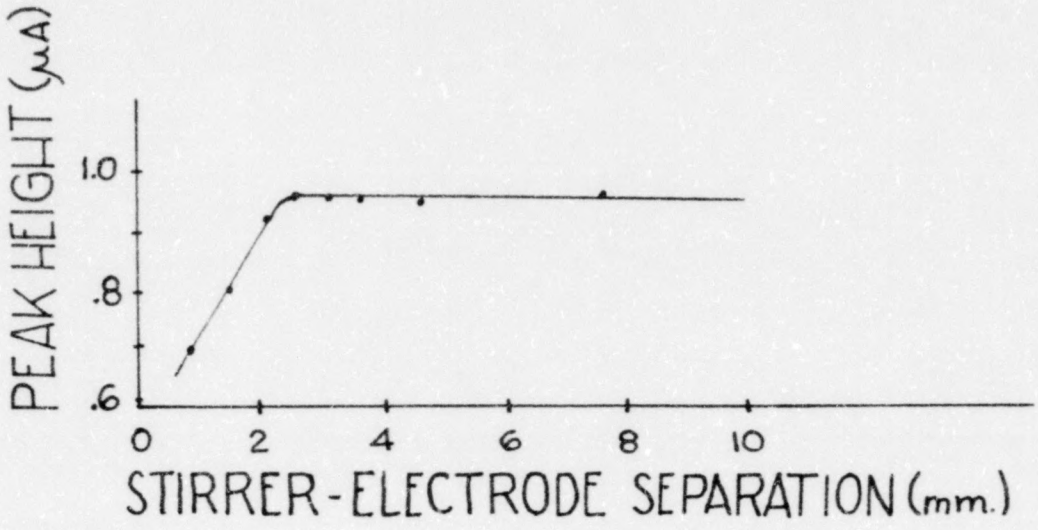

Figure 10. Effect of stirrer-electrode distance on peak values[3]

The effect of mercury drop size on peak-current has shown that, in general, a larger drop is desired[38]. The size of the drop is limited by its ability to remain on the end of the capillary tube of the HDME. Should the drop become too large it will, of course, fall off. Also, since a high stirring rate is desired to speed up the electrolytic concentration (plating) step, the resulting cavitation may also become a factor in shaking the drop off. At the more negative plating potentials, especially above -1.8v (vs. SCE), the surface tension of mercury becomes somewhat lower and its dissolution into the solution is a possibility; the net effect is that the drop becomes more susceptible to being knocked off. Four scale divisions on the mercury microfeeder of the HDME produced a drop which gave excellent results and behaved well. The drop

size was 0.83 mm in diameter or a surface area of 2.22 ± 0.07 mm^2.[38]

Perhaps the most subtle effect on peak current is the length of time allowed for the electrolytic concentration step. If the length of time is too excessive the problem of the analyte diffusing into the capillary tube exists. This will result in the electrode acquiring a "memory" and introducing errors, unless sufficient mercury is extruded from the capillary tube between successive runs. If too little time is allowed the error is also large, as can be seen by analysis of the curve shapes in Figures 11 and 12. Perhaps the best protection against this type of error is through the addition of a standard (standard additions method). Figure 13 shows an actual voltammogram for Cu(II), Pb(II), and Zn(II). On the basis of this curve it was decided that a 5 minute plating time for zinc was desired. For plating times greater than 5 minutes, zinc's behavior is erratic with shifts in the peak potential accompanying a levelling of the peak height.

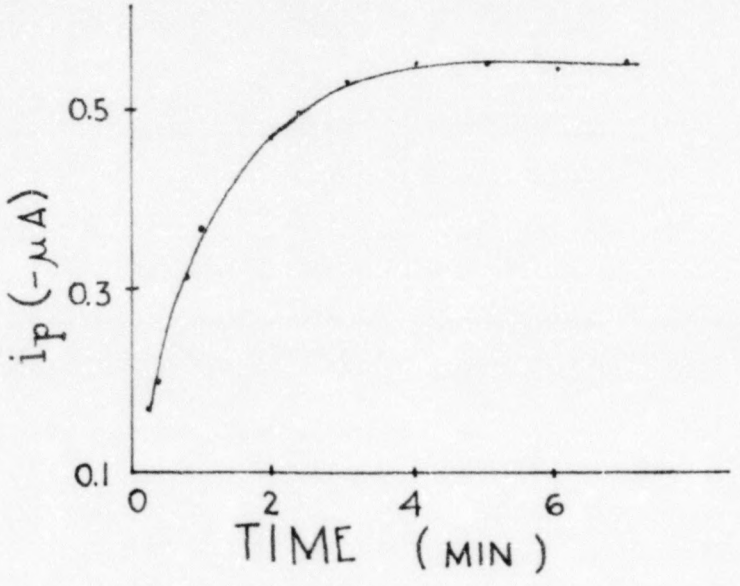

Figure 11. Dependence of Pb(II) peak-current height on time of plating[4]

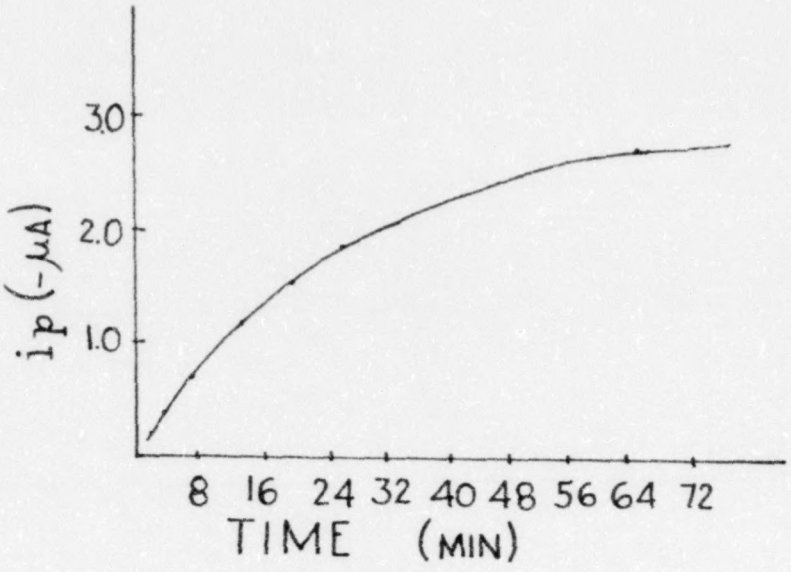

Figure 12. Dependence of Tl^{+} peak-current height on time of Plating[4]

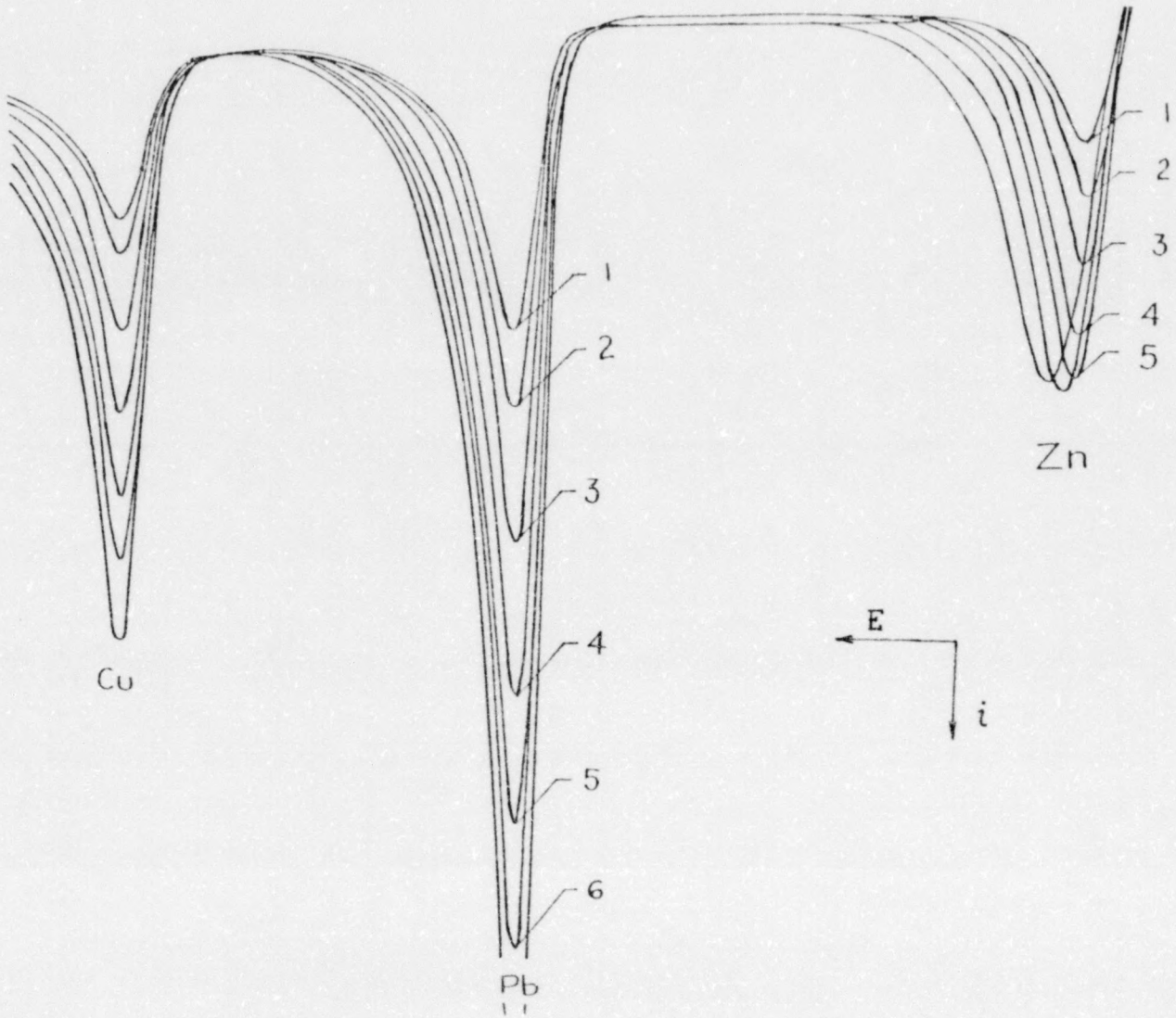

Figure 13. Peak height versus disposition time (min.) at a scan rate of 50 mv/sec for 2 ppm Cu(II), Zn(II), and 10 ppm Pb(II) in 0.1 M KNO_3

The pH of the solution also affects the shape of the dissolution curve as illustrated in Figure 13.[39]

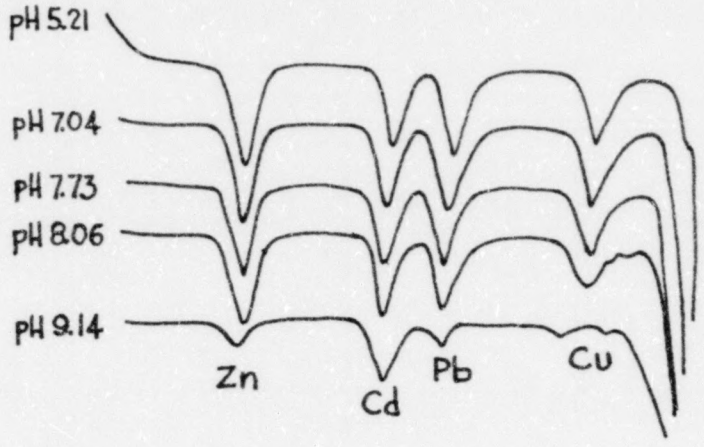

Figure 14. Effect of pH on anodic stripping voltammograms of Zn, Cd, Pb, and Cu.[39]

On the basis of the characteristics of the curves studied thus far it was determined that the conditions best suited for the investigation of the effects that bridging ligands have on the sensitivity of metals using ASV were the following: A 5 minute electrolytic concentration time at a constant potential of -1.4 to -1.5 volts (vs. SCE) followed by a 50 mv/sec anodic scan rate from the plating potential to approximately 0.0 volts (vs. SCE). The 0.0 volt limit was chosen as a protection against mercury oxidation and formation of compounds with the supporting electrolyte. The reproducibility of these conditions was excellent (superimposable), and is illustrated in 5 runs for Zn, Pb, and Cu, as shown in Figure 15.

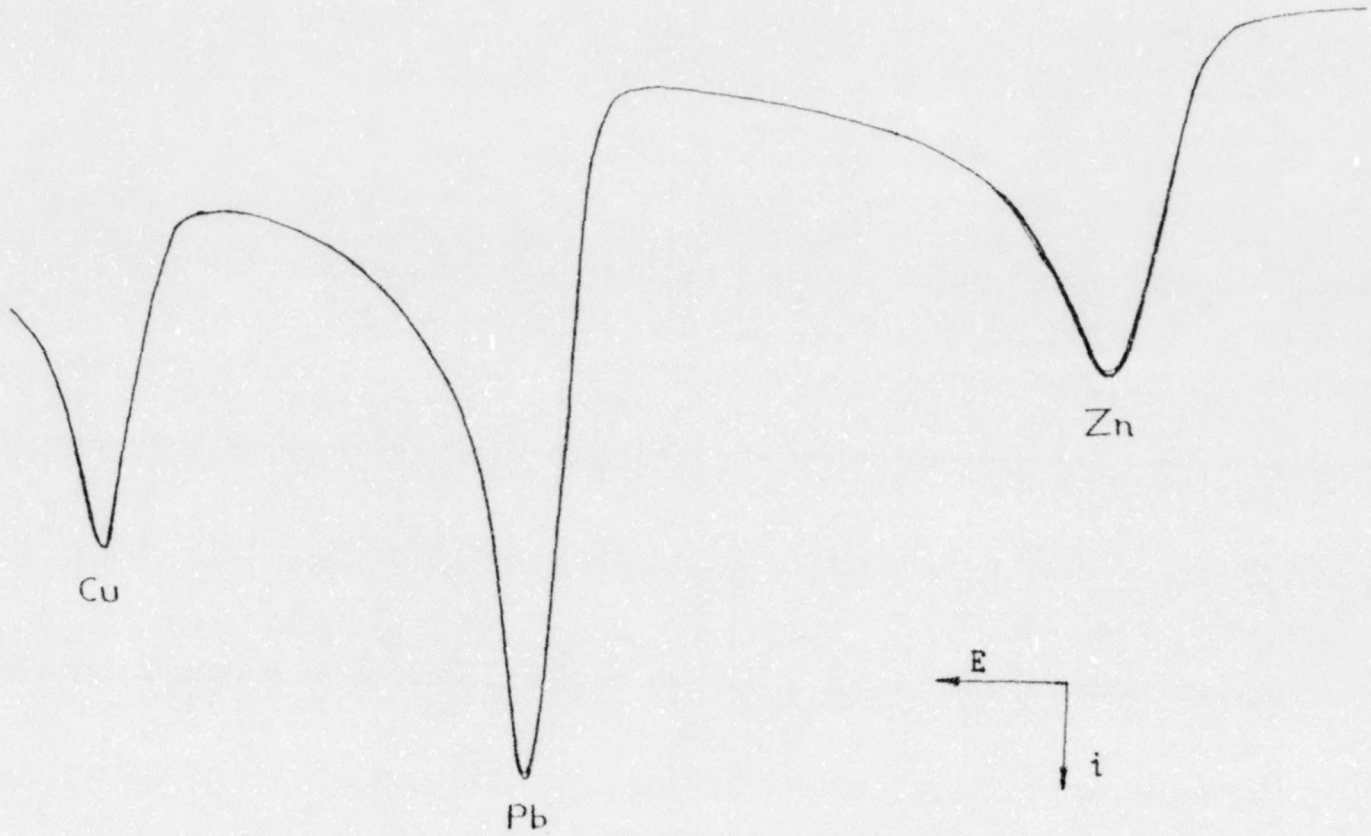

Figure 15. Reproducibility - The result of 5 runs were that they were Superimposable.

B. Effect of Bridging Ligands on Sensitivity

The effect of the addition of bridging ligands to the test solutions exhibited some interesting results. The two ligands added were cyanide (as KCN) and thiocyanate (as KSCN). The exact amount of each ligand added was based on calculations for total complexation as dictated by their association constants, as follows.

For the case of $[Zn(SCN)_4]^{2-}$:

$$Zn^{2+} + 4SCN^- \rightleftharpoons [Zn(SCN)_4]^{2-} \qquad \log \beta_4 = 1.6$$

or, $$\frac{[Zn(SCN)_4]^{2-}}{[Zn^{2+}][SCN^-]^4} = 10^{1.6}$$

if we assume that the metal ion is 99% complexed, leaving only 1% free SCN^- we obtain:

$$\frac{99}{[1][SCN]^4} = \frac{99}{[SCN^-]^4} = 10^{1.6}$$

$$[SCN^-]^4 = \frac{99}{10^{1.6}}$$

$$[SCN^-]^4 = \left[\frac{99}{10^{1.6}}\right]^{1/4} = 1.26 \text{ M } SCN^- \text{ is required to}$$

complex 99% of the zinc as $[Zn(SCN)_4]^{2-}$.

A series of solutions was prepared with the thiocyanate concentration ranging both above and below the 1.26 M value to study the effect of the addition of SCN^- to a zinc solution, with the goal being to increase the peak current significantly.

A similar calculation was performed in the investigation of the cyanide (CN^-) ion:

$$Zn^{2+} + 4CN^- \rightleftharpoons [Zn(CN)_4]^{2-} \qquad \log \beta_4 = 19.7$$

$$\frac{[Zn(CN)_4]^{2-}}{[Zn^{2+}][CN^-]^4} = 10^{19.7}$$

$$\frac{99}{1[CN^-]^4} = 10^{19.7}$$

$$[CN^-] = \frac{99}{10^{19.7}}^{\frac{1}{4}} = 0.0000375 \text{ M}$$

Once again a series of solutions was prepared with the cyanide concentration ranging above and below this value. Similar calculations were done for the other metals. The ionic strength was held constant for each series of ligand solutions so that it would not be a factor in the study. The stability (association) constants for some metals are listed in Table 4.

Table 4

Stability Constants[40]

METAL	SPECIES	LIGAND ADDED		COMMENTS
		CN^-	SCN^-	
Zn(II)	$[Zn(SCN)_4]^{2-}$		$\log \beta_4=1.6$	
	$[Zn(CN_4]^{2-}$	$\log \beta_4=19.7$		
Cd(II)	$[Cd(SCN)_3]^-$		$\log \beta_3=1.9$	
	$[Cd(CN)_4]^{2-}$	$\log \beta_4=18.8$		
Cr(III)	NO INFORMATION AVALIABLE			
Ni(II)	$[Ni(SCN)_3]^-$		$\log \beta_3=1.9$	Nickel can go to $[Ni(CN)]^{3-}$ and $[Ni(CN)_6]^{4-}$ for higher concs. of CN^-.
	$[Ni(CN)_4]^{2-}$	$\log \beta_4=22$		
Co(II)	$[Co(SCN)_4]^{2-}$		$\log \beta_4=2.3$	
	$[Co(CN)_6]^{3-}$	$\log \beta_6=19$		

In view of the similarities between zinc and cadmium, a range of concentrations was chosen that would be suitable for both. As it turned out, the concentrations used were also acceptable for chromium. The results of the ASV studies on solutions of Zn(II), Cd(II), and Cr(III) containing varying concentrations of CN^- and SCN^- are presented in tabular form in Tables 5-7.

In the case of the thiocyanate ligand a problem was encountered where the ASV curve went completely off scale at concentrations of thiocyanate above 1.3 M. Since this also occurred for the SCN^- blank it is assumed this behavior is entirely due to the nature of SCN^- and its interactions with the HDME. It should be noted that in 0.1 M SCN^- (1.4 M KNO_3) the peak current of Zn(II) did apparently increase, at a SCN^- concentration of 0.5 M (1.0 M KNO_3) the peak height was "normal", and at 1.0 M SCN^- (0.5 M KNO_3) the peaks had totally disappeared and the ASV curve was absolutely flat. At concentrations of SCN^- above 1.3 M the ASV curve was again completely off scale. This strange behavior of the SCN^- ligand is not well understood at this time.

Table 5 Data for Zinc

THE BEHAVIOR OF 0.1 ppm ZINC (II)

T=22.2° ± .05°C, E_{el}=-1.5v (vs.SCE), SCAN RATE=50 mv/sec, 5 MIN.ELECTROLYSIS WITH 30 SEC "STILL"TIME

Hg DROP SIZE: 0.83 mm (DIA), 2.22 ± 0.07 mm^2 (SURFACE AREA)

METAL	LIGAND Moles/L	KNO_3 Moles/L	TIME ELAPSED (MIN)	E_p volts vs. (SCE)	i_p (μA)	$\bar{i}_p$ (μA)	$\bar{E}_p$ (volts)
	CN^-						
	.01	.09	36.3	NO PEAKS OBSERVED			
	.001	.099	7.3	NO PEAKS OBSERVED			
	.0001	≈.1	6.9 13.3 19.8 26.3 32.7	-0.984 -0.987 -1.000 -1.005 -1.015	0.410 0.465 0.500 0.600 0.750	0.545	-0.998
	.00001	≈.1	7.0 13.8 23.5 135.5 142.5	-0.980 -0.980 -0.985 -1.005 -1.013	0.455 0.780 0.760 0.430 0.460	0.577	-0.993
	.000001	≈.1	7.0 13.3 20.8 28.8 35.2 41.5 47.7	-0.982 -0.982 -0.982 -0.982 -0.982 -0.982 -0.982	0.580 0.652 0.680 0.768 0.664 0.730 0.795	0.695	-0.982
	0.0	0.1	7.3 17.8 24.0 30.4	-0.905* -0.920 -0.918 -0.918	0.538 0.528 0.492 0.483	0.522	-0.919
	0.0	1.5	7.0 14.0 21.0 27.5 35.3 52.5	-0.972 -0.972 -0.980 -0.972 -0.967 -0.965	0.395 0.360 0.500 0.250 0.083 1.025*	0.318	-0.971
	SCN^-						
	.1	1.4		-0.987 -0.987 -0.987	1.368 1.345 1.385	1.366	-0.987
	.5	1.0		-1.035 -1.035 -1.035 -1.035	0.590* 0.485 0.485 0.485	0.487	-1.035
	1.0	.5	THE PEAKS HAVE GONE, SPECTRUM IS TOTALLY FLAT				
	1.3	.2	THE ENTIRE SPECTRUM IS OFF SCALE				
	1.5	0.0	THE ENTIRE SPECTRUM IS OFF SCALE				

*Not Averaged.

Table 6 Data for Cadmium

BEHAVIOR OF .1 ppm CADMIUM(II)

T=2.22°C±.05, E_{el}=-1.4v (vs SCE), SCAN RATE=50mv/sec, 5 MIN ELECTROLYSIS WITH 30 SEC.STILL TIME

Hg DROP SIZE: 0.83 mm (DIA), 2.22 ± 0.07 mm^2 (SURFACE AREA)

METAL	LIGAND Moles/L	KNO_3 Moles/L	TIME ELAPSED MIN.	E_p (volts vs.SCE)	i_p µA	$\bar{I}_p$	$\bar{E}_p$
	CN						
	.01	0.9	5.5 12.4 18.7 25.5 33.2	-0.755 -0.755 -0.755 -0.755 -0.755	* 0.286 0.290 0.288 0.265	0.288	-0.755
	.001	.099	5.5 12.4 18.8 25.3 32.2	-0.625 -0.625 -0.625 -0.625 -0.625	0.263 0.360 0.305 0.300 0.330	0.300	-0.625
	.0001	~.1	8.1 14.8 22.3 28.9 37.1	-0.562 -0.562 -0.563 -0.563 -0.564	0.388 0.400 0.430 0.375 0.365	0.392	-0.563
	.00001	~.1	7.3 13.9 22.3 28.7 35.3 49.6	-0.562 -0.562 -0.562 -0.562 -0.562 -0.562	0.253 0.293 0.293 0.3375 * 0.3275	0.301	-0.562
	.000001	~.1	7.0 13.3 19.8 26.3 33.9 40.5 48.6	-0.562 -0.562 -0.562 -0.562 -0.562 -0.562 -0.562	0.180 0.180 0.209 0.294 0.363 * 0.415	0.274	-0.562
	0.0	0.1	7.25 13.8 21.0 28.1	-0.557 -0.557 -0.557 -0.557	0.549 0.562 0.562 *	0.558	-0.557
	0.0	1.5	8.0 14.4 23.6	-0.562 -0.562 -0.562	0.757 0.975 0.630	0.7872	-0.562
	SCN^-						
	.1	1.4	ALL PEAKS (BASELINE) GO FLAT AFTER SCN^- IS ADDED				

*Value not averaged.

Table 7 Data for Chromium

THE BEHAVIOR OF 9.9 ppm CHROMIUM(III)

T = 22.2 ± 0.05°C, E_{el} = -1.5v (vs SCE), SCAN RATE = 50mv/sec, 5 MIN. ELECTROLYSIS WITH 30 SEC STILL TIME

Hg DROP SIZE: 0.83 mm (DIA), 2.22 ± 0.07 mm^2 (SURFACE AREA)

METAL	LIGAND Moles/L	KNO_3 Moles/L	TIME ELAPSED (MIN)	E_p Volts vs SCE	i_p µA	$\bar{i}_p$ µA	$\bar{E}_p$ volts
	CN^-						
	.01	.09	13.0	NONE FOUND	NONE FOUND	"WHITE CLOUD" FORMED UPON THE ADDITION OF CN^- (PPT↓?)	
	.001	.009	6.8 13.2	-1.155 NONE	0.120 NONE	?	?
			NOTE: THE WHITE MILKY CLOUD FORMED MORE GRADUALLY THAN WITH .01 M CN^-; RESULT-PEAK DISAPPEARED WITH TIME.				
	.0001	~.1	7.5 16.3 22.2 48.4	-1.067 -1.065 -1.053 -1.050	0.210 0.247 0.393 0.475	0.331	-1.059
	.00001	~.1	14.1 20.4 27.0	-1.057 -1.057 -1.057	0.218 0.220 0.220	0.219	-1.057
	.000001	~.1	12.9 19.7 35.2	-1.062 -1.062 -1.062	0.155 0.160 0.165	0.160	-1.062
	0.0	0.1	16.8 23.3 46.3	-1.050 -1.055 -1.040	0.270 0.270 0.345	0.270	-1.048
	0.0	1.5	8.0 16.5 22.0 29.0 35.3	-1.027 -1.027 -1.010 -1.010 -1.010	0.090 0.135 0.268 -.373 0.455	0.264	-1.0168
	SCN^-						
	0.1 0.5	1.4 1.0	NO PEAKS OBSERVED (EVEN FLATTENED OUT BASELINE) UPON ADDITION OF SCN^- LIGAND				

Upon examination of the data in these tables, some obvious effects of CN^- and SCN^- on the ASV analysis of Zn(II), Cd(II), and Cr(III) can be noted. The peak potentials, E_p, are shifted cathodically compared to the peak potentials of the metals in the KNO_3 supporting electrolyte. A cathodic shift in the peak potentials for the three metal ions is also observed with increasing concentration of the ligands. The conclusion is that the complex species the metals form with CN^- and SCN^- are more difficult to reduce, or the reduced species are more easily oxidized from the mercury electrode when the ligands are present.

As indicated by the data in tables 4-6, the peak currents are variable with increasing ligand concentration. No ASV curves were obtained for Zn(II) with concentrations of CN^- above 0.001 M and SCN^- above 1.0 M, Cd(II) with concentrations of SCN^- above 0.1 M, and Cr(III) with concentrations of CN^- above 0.001 M and SCN^- above 0.1 M. In these cases the concentration of the ligand approaches the concentration necessary for total complexation of the metal. When the metal is totally complexed, the species acquires an overall negative charge and may be repelled by the negatively charged HDME.

Initially it was hoped that the bridging ligands, SCN^- and CN^- would bond to the mercury electrode in the manner illustrated in Fig. 16. In the case of the thiocyanate ion, the metals used in this study bond to this ligand through the nitrogen atom. This leaves the sulfur atom free to bridge to the mercury in the HDME. According to the "hard soft acid base theory" both the sulfur and mercury atoms are "soft" and

bonding between them is favored. Since SCN^- is capable of promoting electron transfer reactions, it was thought that this property along with the possibility of bridging between the complex species and the electrode would increase the sensitivity of the metal ions in ASV analysis.

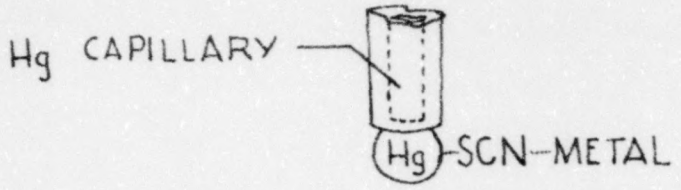

Figure 16. Desired bridging between HDME and metal ion

In the case of zinc it would seem this did occur until total complexation apparently took place, When cyanide was used as a ligand no peak current was observed at the higher concentrations (.01 M, .001 M). At concentrations of CN^- below 0.001 M the peak currents did increase. An increase of peak currents with time was also observed which indicated an electrode memory effect. However, in between several of the runs, mercury was extruded from the capillary (approximately half the column height) and the increase with time was still noted. This increase in time is plotted for some selected concentrations in Figures 17 and 18. The working curve for zinc (Fig. 19) indicates a well-behaved nature, whereas the peak current vs. ligand (CN^-) concentration curve has rather significant ranges (Fig. 20). In general, peak current decreased with increasing CN^- concentration in a slightly less than linear fashion.

Cadmium and chromium(III) exhibit a maximum value of peak current (Figs. 21 and 22) at .00001 M CN^-. The working

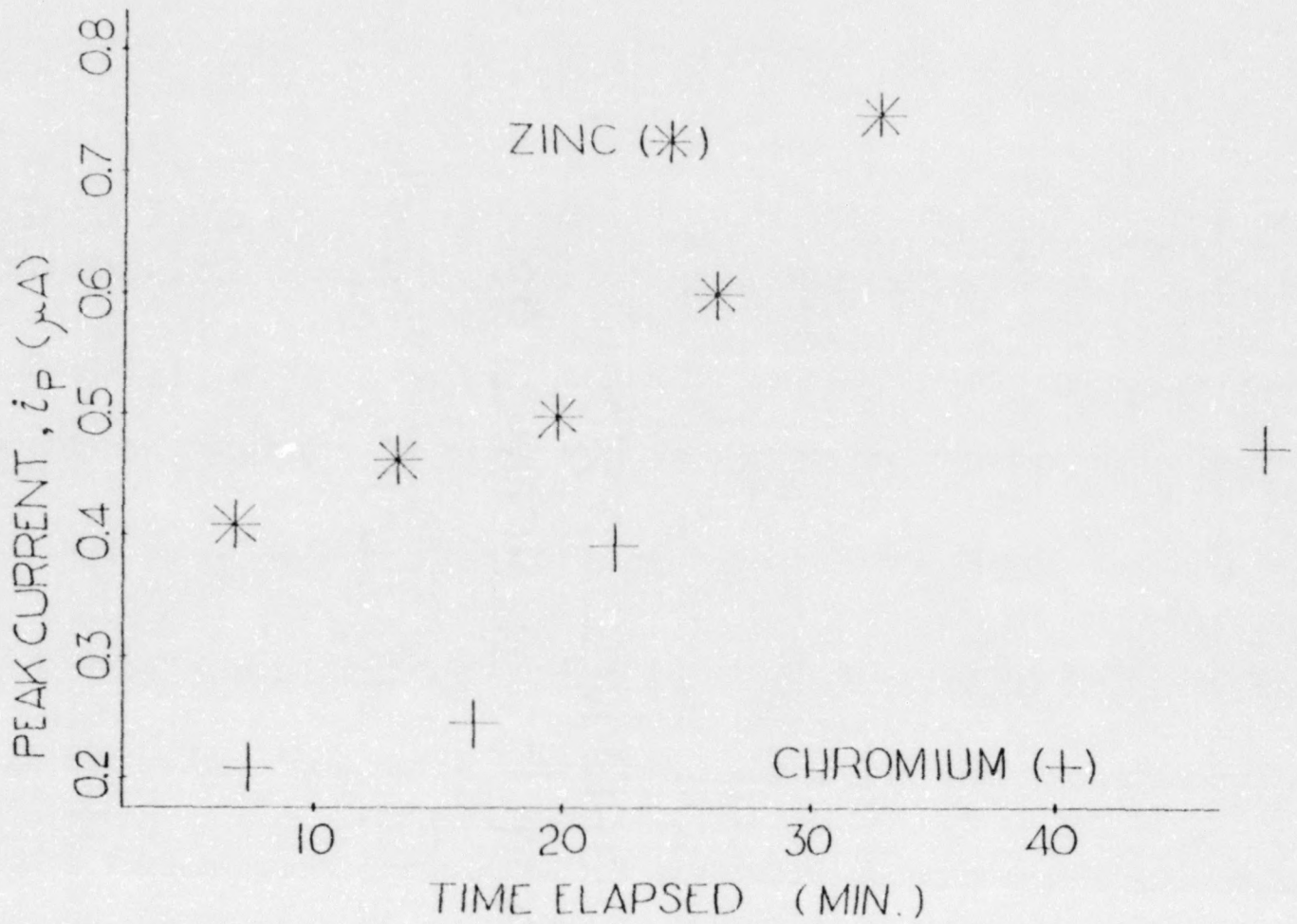

Figure 17. Peak current versus time elapsed for 9.9 ppm Cr(III) and 0.1 ppm Zn(II) in a 0.0001 M CN^- - 0.1 M KNO_3 solution.

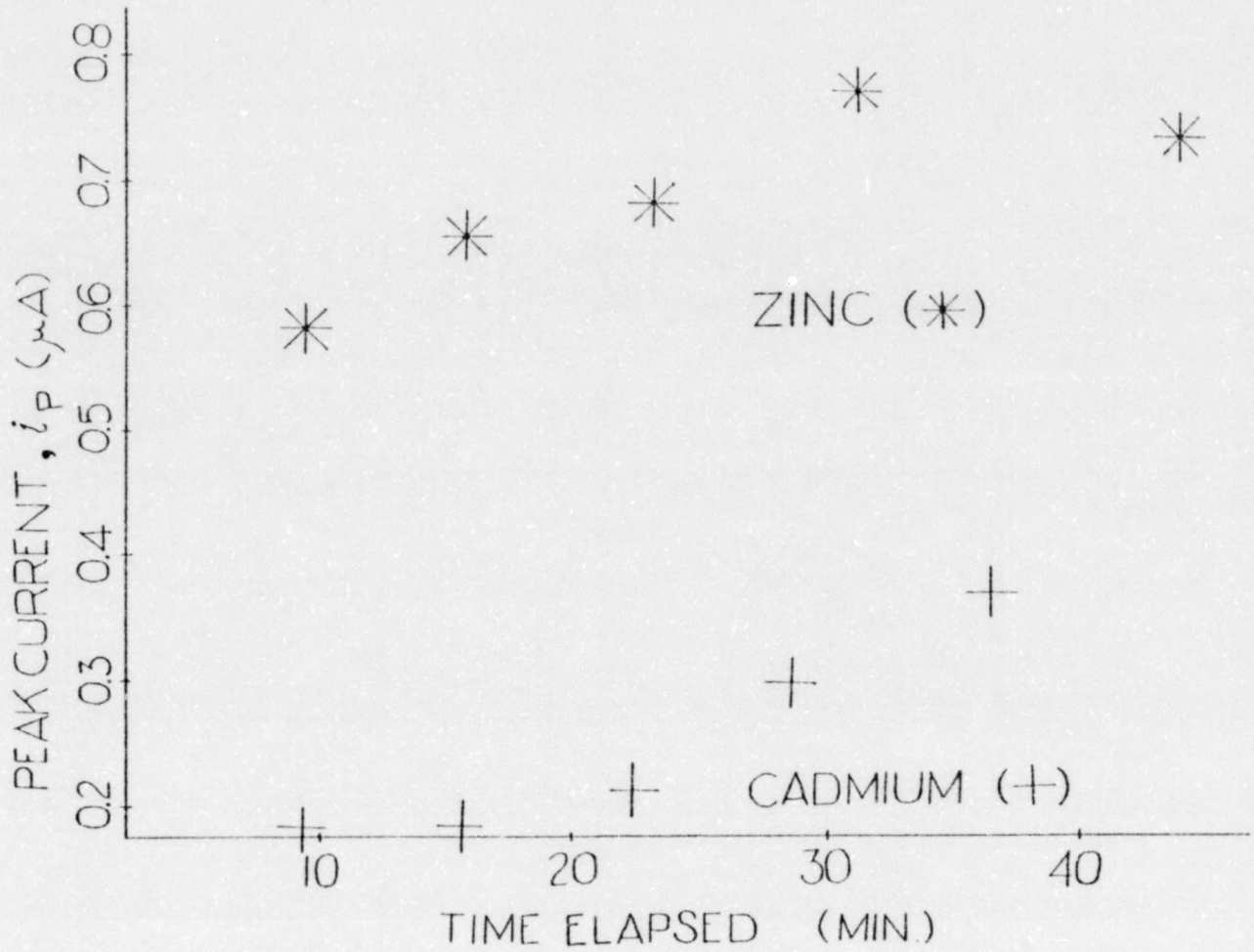

Figure 18. Peak current versus time elapsed for 0.1 ppm Cd(II) and Zn(II) in a 0.000001 M CN^- - 0.1 M KNO_3 solution.

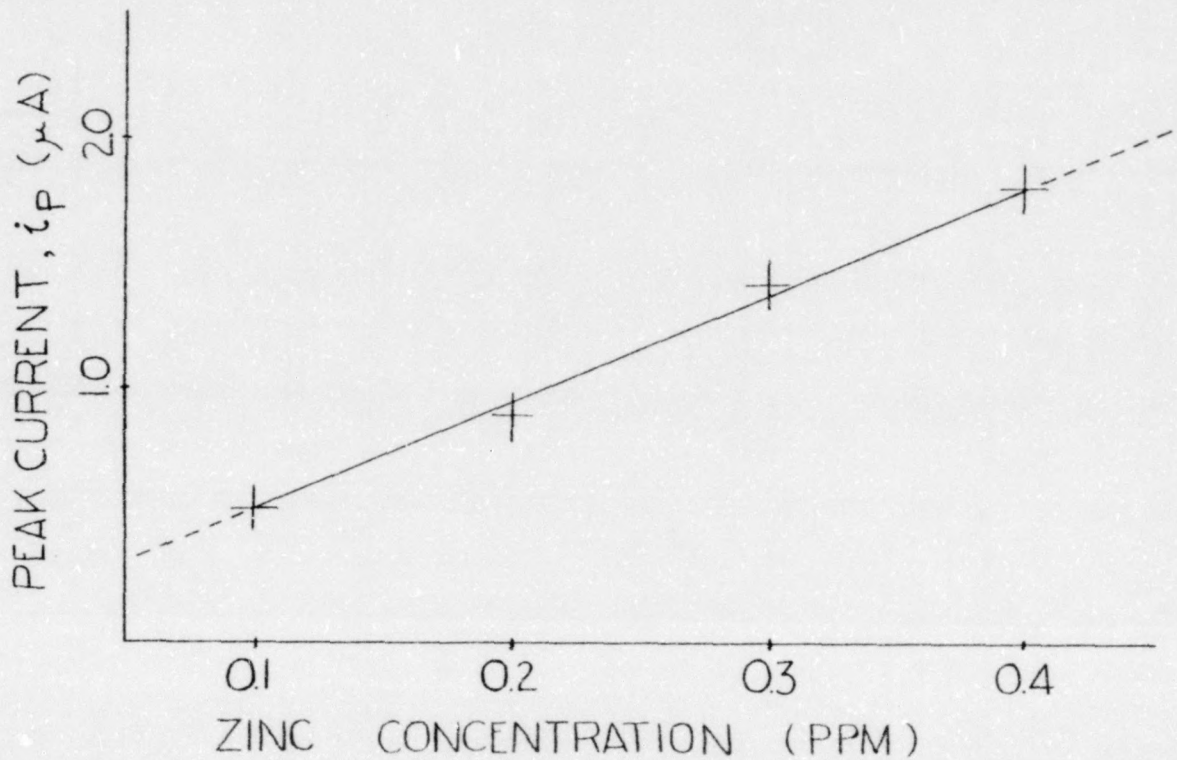

Figure 19. The zinc working curve in 0.1 M KNO_3

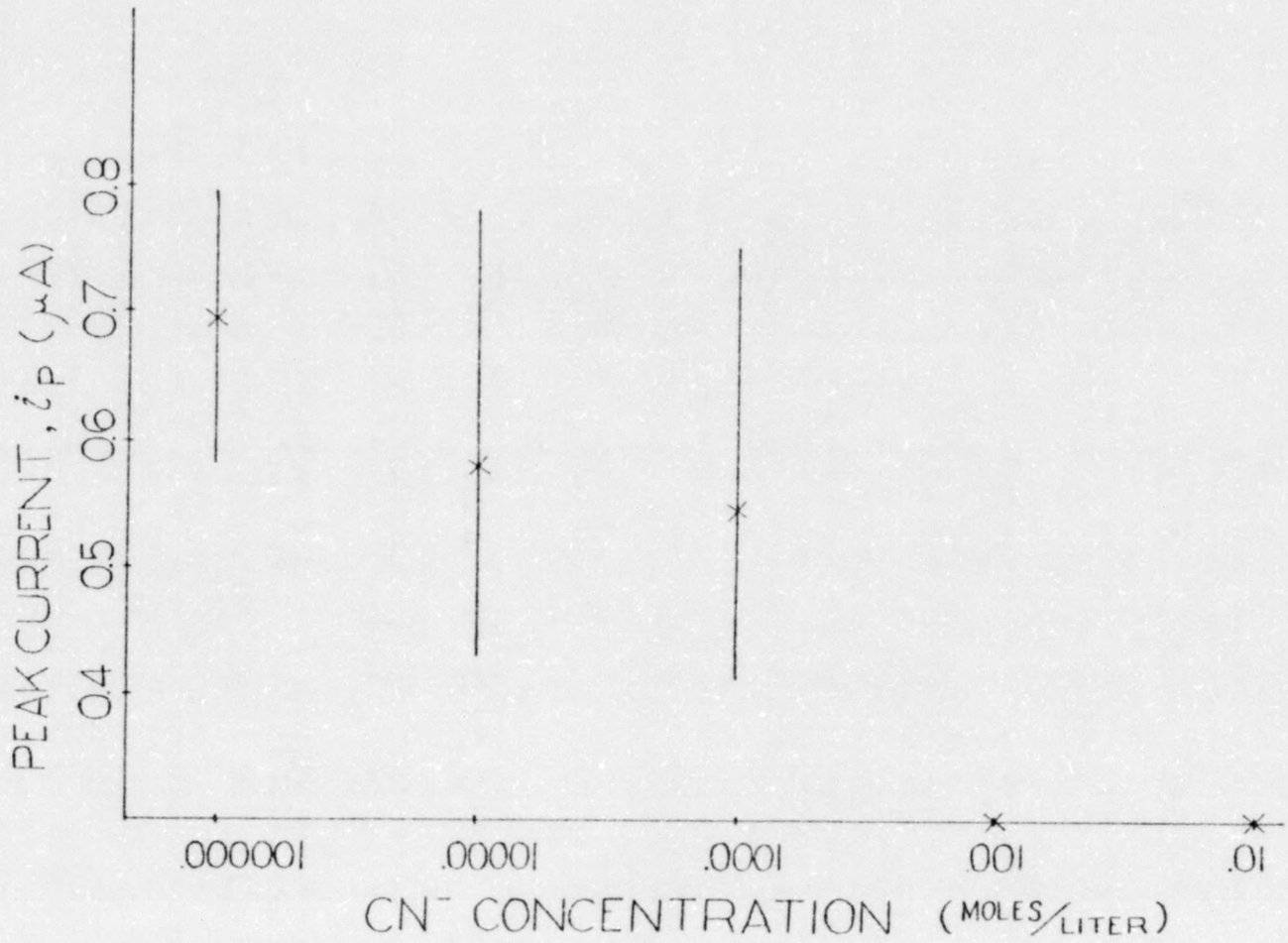

Figure 20. Peak current versus CN^- concentration for 0.1 ppm Zn(II) in 0.1 M KNO_3

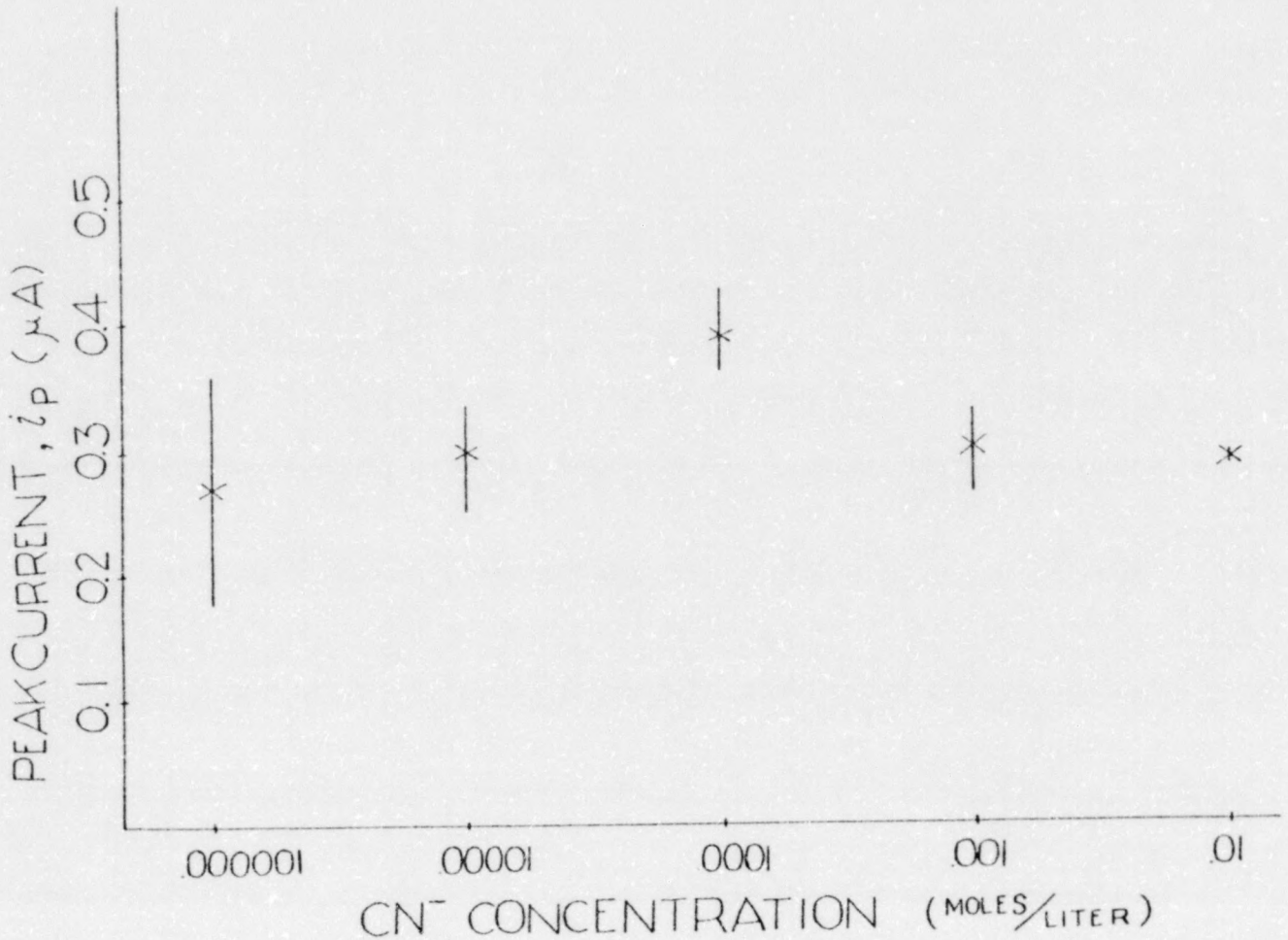

Figure 21. Peak current versus CN^- concentration for 0.1 ppm Cd(II) in 0.1 M KNO_3

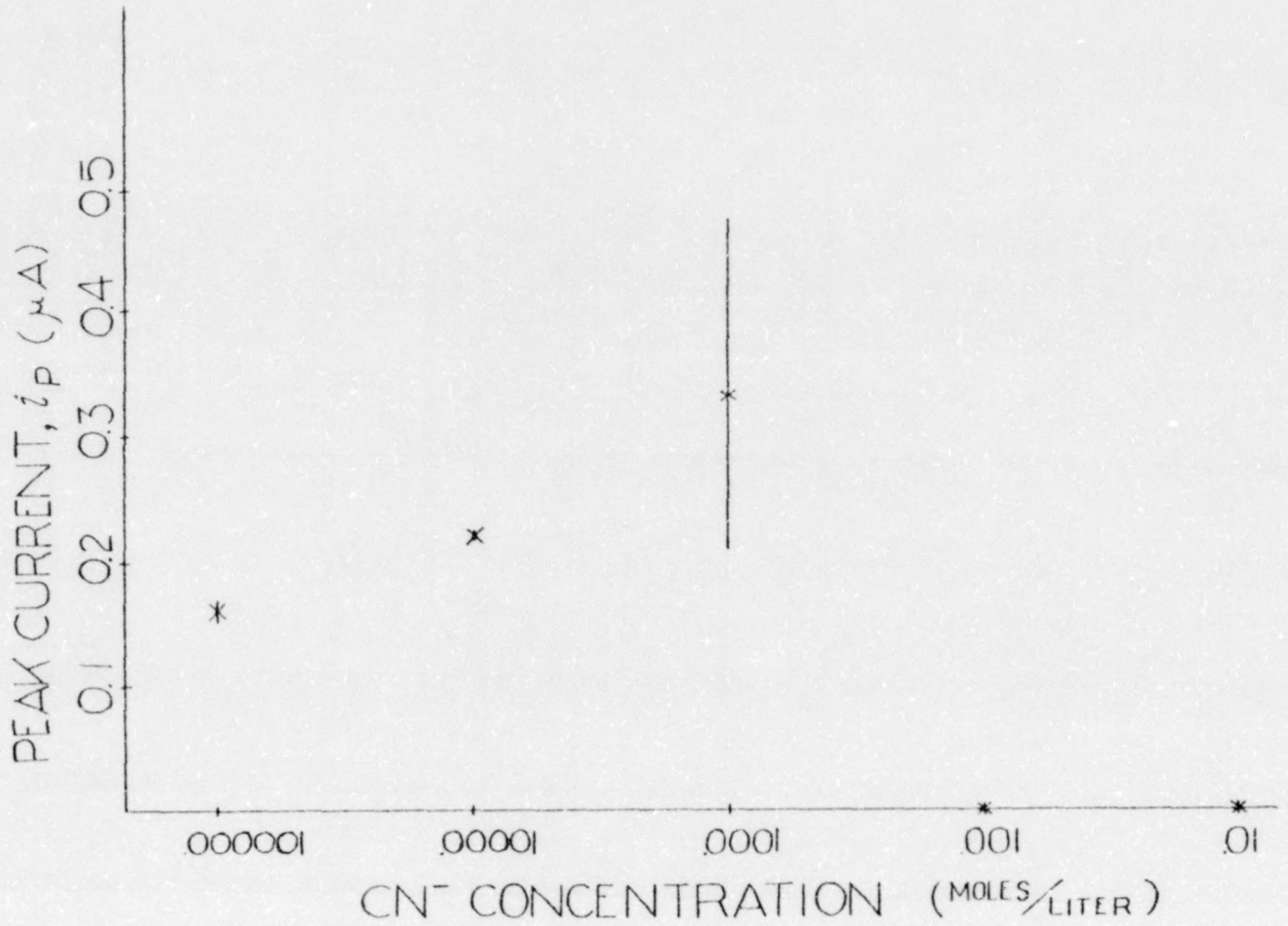

Figure 22. Peak current versus concentration for 0.0 ppm Cr(III) in 0.1 M KNO_3

curve for Cd(II) is linear,[37] however, the variation of peak current is non-linear. The peak current increases (only slightly) with increasing concentration of CN^- up to the point where total complexation is predicted. Beyond this value (greater than 0.0001 M CN^-), the peak current begins to show a steady decrease, as if the excess of cyanide ligand prevents the detection of the metal complex at the electrode's surface.

Chromium exhibited a rather odd dissolution curve shape unlike any of the others. The difference is immediately visible in Fig. 23 as an inflection.

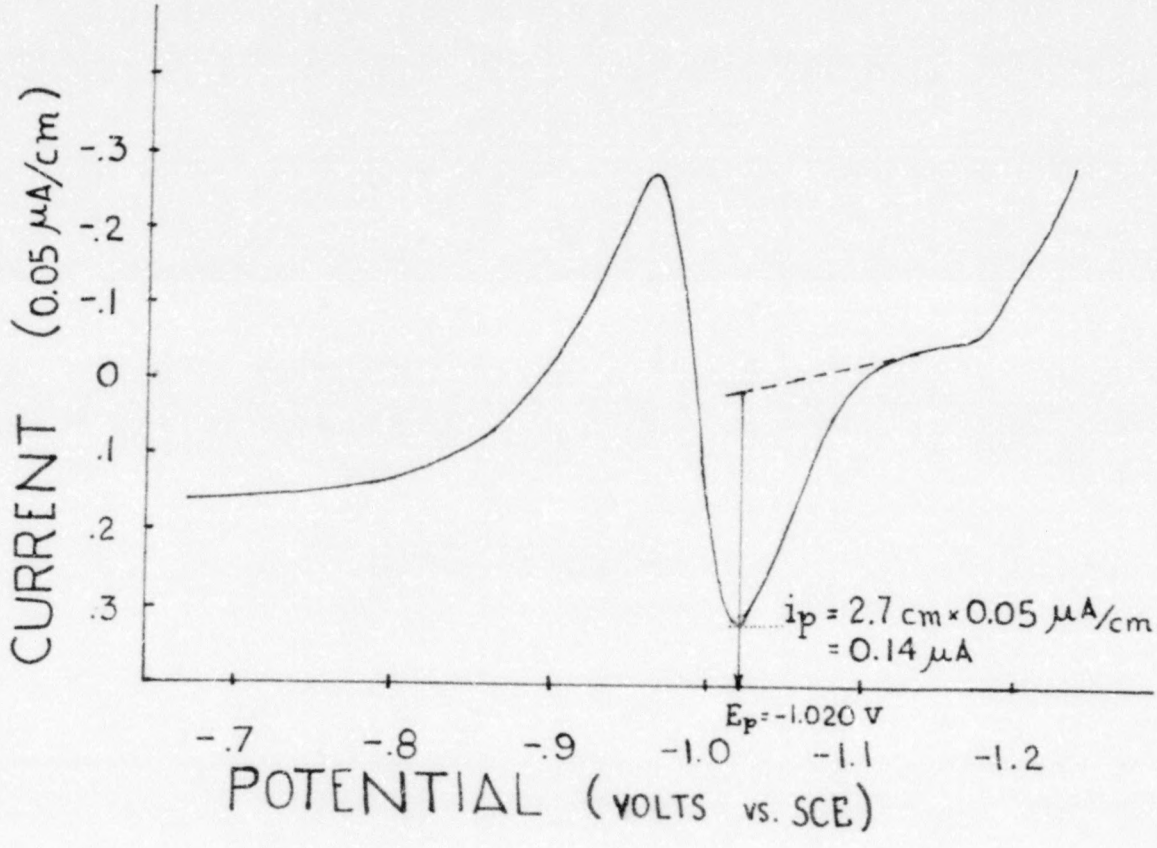

Figure 23. Dissolution curve for 9.9 ppm Cr(III) in 1.5 M KNO_3

The reason for this curve shape is not understood at this time. It did occur with all the Cr(III) solutions and one can only conclude it is the nature of chromium causing this unusual behavior. An increase in peak-current with increasing concentration was observed up to the point of total complexation (0.001 M CN^-) where a "milky white cloud" was observed to form slowly when Cr(III) was added to the solution. This "cloudy" formation was observed to occur even more rapidly for the higher cyanide concentration (.01 M). At both of these concentrations (.001 M and .01 M CN^-) there was no peak observed. Even the background run had been flattened out, as if there were no current flowing between the electrodes immersed in the solution. This was the same condition observed in the previous runs for zinc and cadmium (with SCN^- also). It may be that the deactivated species formed by complexation surrounds the electrode so that no charges can successfully approach it.

Attempts were made to include Co(II), Ni(II) and Fe(II) in this study. However, it was found that these metals exhibited no detectable peaks within the range of voltages selected. For Fe(II), this problem was attributed to the metal's inability to form an amalgam with the HDME.

In general, the addition of the cyanide or thiocyanate ligand did not appreciably enhance the peak-currents sufficiently to consider their addition beneficial to detecting the metals (Zn, Cd, Cr) at more dilute concentrations than by present methods. It might do well to investigate neutral ligands, such as NH_3, and determine their effects, since they might promote bringing a complexed metal to the negative electrode

more effectively (or at least to the Nernst diffusion layer).

As a matter of interest, the metals which are currently easily detected by anodic stripping voltammetry appear in Fig. 24. Notice that chromium does not appear in this chart. This research was an attempt to place it there with some degree of confidence. However, there still is room for improvement and understanding.

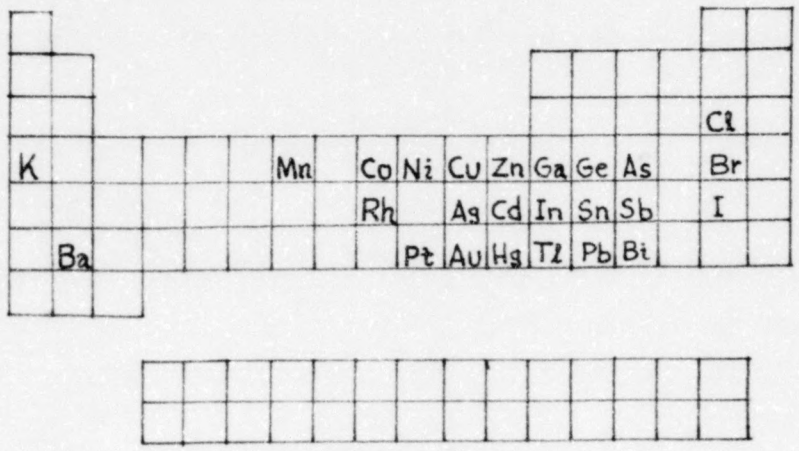

Figure 24. Elements determined by stripping voltammetry[39]

In summary, the effect of increasing ligand concentration was to increase the peak current until the point of total complexation was reached. At this point the peak current began to decrease with further ligand addition. The increase in peak current was not as great as hoped for at the outset of this research project, with the possible exception of the combination of 1.0 M SCN^- and 1.4 M KNO_3, which resulted in approximately a three-fold increase in the peak current for zinc(II). As an analytical technique, it would seem that the addition of cyanide ligand is not very promising, and

thiocyanate seems unsuited for use with the HDME-KNO_3 electrolyte combination. One interesting result was that higher ionic strengths seemed to do more for peak current enhancement than the addition of ligands such as cyanide (compare the i_p values for .1 M KNO_3 vs. 1.5 M KNO_3).

Investigations into SCN^- ligand addition for different electrodes such as the WIGE and GPE may show improvement in its use as an analytical tool. Different electrolytes may also improve the sensitivity of this method, $KClO_4$ and KBr have been tried and are not too well suited to the technique. When KBr is added under appropriate conditions with the HDME Hg_2Br_2 forms in the analyzing solution causing its contamination. Finally, the addition of neutral ligands, such as NH_3, should be tried in the hope that the positively charged complexes that form may enable them to reach the working electrode more efficiently and thereby increase the sensitivity of the metal.

BIBLIOGRAPHY

1. Zbinden, C., Bull. Soc. Chim. Biol., 13, 35 (1931).

2. R. D. DeMars and I. Shain, Anal. Chem., 29, 1825 (1957).

3. J. G. Nikelly and W. D. Cooke, Anal. Chem. 29, 933 (1957).

4. L. Huderova and K. Stulik, Talanta, 19, 1285 (1972).

5. V. Frantisek, K. S. Tulik, E. Julakova, "Electrochemical Stripping Analysis," Halsted Press/John Wiley & Sons, Inc., 605 3rd Ave., NY, NY 10001 (1976).

6. T. R. Copeland, R. K. Skogerbec, Anal. Chem., 46, No. 14, 12574 (1974).

7. T. R. Copeland, J. H. Christie, R. A. Osteryoung, R. K. Skogerboc, Anal. Chem., 45, 2171 (1973).

8. L. Zieglerova, K. Stulik, J. Dolezal, Talanta, 18, 603 (1971).

9. M. Kopanica, F. Vydra, J. Electroanal. Chem., 31, 175 (1971).

10. W. Kossel, Nachr. Geo. Wiss. Gottingen, Math-Physik. Kl., 175 (1927). Reference 5 summarizes this work.

11. I. N. Stranski, Z. Physik. Chem., 136A, 259 (1928); Naturwiss, 37, 289 (1950). Reference 5 summarizes this work.

12. M. Volmer, "Die Kinetik der Phasenbildung," Steinkopff, Dresden, Leipzig (1939). Reference 5 summarizes this work.

13. M. Volmer, Z. Physik Chem., 102, 267 (1922). Reference 5 summarizes this work.

14. T. Erdey-Gruz and M. Volmer, Z. Physik Chem., 157A, 165 (1931). Reference 5 summarizes this work.

15. M. Fleischman, H. R. Thirsk, "Advances in Electrochemistry and Electrochemical," ed. P. Delahay and C. W. Tobias, Vol. 3, p. 123, Interscience, New York (1963).

16. W. K. Burton, N. Cabrera, F. C. Frank, Nature, 163, 398 (1949).

17. W. K. Burton, N. Cabrera, F. C. Frank, Phil. Trans. Roy. Soc., 243A, 299 (1951).

18. M. T. Kolzlovskii, A. I. Zebiern, V. P. Gladyshev, "Amalgamy i ikh Primenenic," lzd, Nauka, Alma-Ata (1971). Reference 5 summarizes this work.

19. V. P. Gladyshev, Vestn. AN Kaz SSR, 11, 53 (1963). Reference 5 summarizes this work.

20. F. A. Cotton, G. Wilkinson, "Advanced Inorganic Chemistry - A Comprehensive Text," p. 836, 3rd Ed., Interscience, (1972).

21. K. Jones, R. B. Heslop, "Inorganic Chemistry - A Guide to Advanced Study," p. 592, Elsevier Scientific Publishing Compnay (1976).

22. C. F. Bell, "Metal Chelation - Principles and Applications," p. 39, Clarendon Press, Oxford (1977).

23. P. Delahay, "New Instrumental Methods in Electrochemistry," 115-145, Interscience, New York, NY (1955).

24. W. T. deVries, E. Van Dalen, J. Electroanal. Chem., 14, 315 (1967).

25. E. Barendrecht, "Electroanalytical Chemistry," A. J. Bard, Ed., Vol. II, Marcel Dekker, New York, NY (1967).

26. W. D. Ellis, J. Chem. Ed., 50, A131 (1973).

27. W. H. Reinmuth, Anal. Chem., 33, 185 (1961)

28. I. Shain, J. Lewinson, Anal. Chem., 33, 187 (1961).

29. D. K. Roe, G.E.A. Toni, Anal. Chem., 37, 1503 (1965).

30. N. Velghe, A. Claeys, J. Electroanal. Chem., 35, 229 (1972).

31. W. T. deVries, J. Electroanal. Chem., 9, 448 (1965).

32. A. Sevik, Collection Czechoslov. Chem. Communs., 13, 349 (1948). Reference 5 summarizes this work.

33. J.E.B. Randles, Trans. Faraday Soc., 44, 327 (1948).

34. M. M. Nicholson, J. Am. Chem. Soc., 76, 2539 (1954).

35. A. A. Noyes, W. R. Whitney, Z. Physik. Chem., 23, 689 (1897). Reference 5 summarizes this work.

36. W. Nernst, Z. Physik. Chem., 47, 52 (1904). Reference 5 summarizes this work.

37. G. Colovas, G. S. Wilson, J. Moyers, Analytica Chimica Acta, 64, 460 (1973). Reference 5 summarizes this work.

38. Inverse Polarography (anodic stripping) operating instructions, Metrohm Herisau, Switzerland.

39. F.P.J. Cahill, G. W. VanLoon, American Laboratory, 11, Aug. (1976).

40. Meites, "Handbook of Analytical Chemistry," Table 1-17, pp. 1-39, McGraw Hill, New York, NY (1963).